공학석사학위 논문

Novel Photochromic and Piezochromic Fluorescence Smart Materials Based on Highly Emissive Dicyanodistyrylbenzene Derivatives: Studies on Photophysical Properties, Stimuli-Responsive Luminescence Changing Behavior, and Their Crystal Structure

고형광성 다이사이아노스틸벤 파생물들을 기반의 새로운 압력변색성 광응답성 스마트형광소재: 광물리적 특성, 자극에 의한 광 변화, 그리고 결정구조에 대한 연구

2013 년 8 월

서울대학교 대학원

재료공학부

정 재 훈

Novel Photochromic and Piezochromic Fluorescence Smart Materials Based on Highly Emissive Dicyanodistyrylbenzene Derivatives: Studies on Photophysical Properties, Stimuli-Responsive Luminescence Changing Behavior, and Their Crystal Structure

고형광성 다이사이아노스틸벤 파생물들을 기반의 새로운 압력변색성 광응답성 스마트형광소재: 광물리적 특성, 자극에 의한 광 변화, 그리고 결정구조에 대한 연구

지도교수 박 수 영

이 논문을 공학석사 학위논문으로 제출함

2013 년 8 월

서울대학교 대학원

재료공학부

정 재 훈

정재훈의 석사학위논문을 인준

Abstract

Novel Photochromic and Piezochromic Fluorescence Smart Materials Based on Highly Emissive Dicyanodistyrylbenzene Derivatives: Studies on Photophysical Properties, Stimuli-Responsive Luminescence Changing Behavior, and Their Crystal Structure

Jaehun Jung
Department of Materials Science and Engineering
The Graduate School
Seoul National University

Solid-state mechanical stimuli responsive organic materials are a promosing avenue of research in crystal engineering and for a wide range of application such as fluoresent sensor, optical memory device, and secret paper. Despite those intensive reseach, the

design strategy to controll molecualr packing and their optical properties is very limited. Also the theoretical understanding of luminescent switching by changing molecular assembly at molecular level and the correlation of structure-optical property remains still unclear. Recently, a lot of mechanochromism materials were reported and investigated to aware the role of molecular stacking in determining solid-state optical properties of π-conjugated materials. Neverthless, at the current stage, only a few group explained the structure-optical property relationship and the mechanism of structure change by stimuli successfully.

Herein, I report on a novel class of α-dicyanodistyrylbenzene derivatives exhibiting distinct characteristics, i.e, (i) aggregation-induced enhanced emission (AIEE) behavior, (ii) polymorph and polymorph-dependent emission behavior, (iii) mechanical and solvent vapor stimuli induced fluorescence change and thermal induced recovery, (iv) isomerization E(Z)-form to Z(E)-form, especially in the mechanical perturbed solid state under UV-light. The molecules structures are very similar except the length of alkoxy-chaing and position of cyano-group. Although the molecules′ backbonds deteriminate intrinsic photophysical properties, the optical properties and stimuli-responsive behavior are quite different. In this respect, to understand various optical performance in solid state, I study followings: (i) the role of length of alkoxy chain and position of cyano-group to controll crystal structrue and optical properties (ii) in-depth understanding of the mechanism of fluorescence quenching only at mechanically

perturbed state. From crystal structure analysis, measurement photophysical properties, XRD, and ^{1}H-NMR data, I suggest the most plausible mechanism of the unique phenomena and the theoretical explanation of the structure-optical properties relationship. Finally, I demonstrated reverisble piezo-writing and read-out-only(ROM) processable memory device.

Keywords: dicyanodistyrylbenzene, piezochromism, mechanochromism, molecular assembly, photoisomerization, fluorecence writing, Crystal Engineering

Studnet Number: 2011-2405

Contents

List of Tables

List of Schemes

List of Figures

Chapter 1. Introduction

1.1 Aggregation-induced enhanced emission(AIEE)

The optical and electronic properties in solid state of planer Π-conjugated molecules are defined by not only the chemical structure of molecules but also the electronic coupling by the intermolecular interactions. Strong π-π interaction between neighboring molecules promotes delocalization of the polarons/exciton which increase charge carrier mobilities.[1] However, the interaction creates new non-radiative decay pathway of excitons which compete with emissive routes. Commonly, Π-conjugated molecules show solid-state luminescence quenching of which phenomena is referred as concentration quenching. [2]

Compared to common planer Π-conjugated molecules such as stilbene, some cyanostilbene derivatives show highly fluorescence in solid state but weak fluorescence in solution state, which called aggregation-induced enhanced emission (AIEE). The main reason of the different phenomena is orientation of molecules in aggregation state. For the majority of Π-conjugated molecules including stilbene, the molecular dipole moment μ is mainly oriented along the long molecular axis (Figure 1.1). When molecules are oriented by head-to-head, we call H-aggregation. In H-aggregation state, the higher transition state generated by electronic coupling is dipole moment transition allowed state. However, the lower transition state is forbidden state due to zero net transition dipoles. The absorption spectra is hypsochromically(blue) shift against the solution. In accordance with Kasha's rule, transition to ground state is mainly S1 -> S0 transition. The lower transition state to ground state transition is also forbidden and thus H-

aggregates frequently show weak fluorescence and result in concentration quenching, which is observed for the majority of Π-conjugated molecules in the solid state. In contrast, J-type stacking molecules are oriented by head-to-tail. The higher transition state generated by electronic coupling is forbidden states due to zero net transition dipoles. In contrast, the lower transition state is allowed states. Therefore the absorption spectra are bathchromically(red) shift from solution and the molecule exhibits high radiative rate constants K_f. Even thought the molecules do not present fluorescence in solution, J-aggregates can show highly luminescence, so-called aggregation-induced enhanced emission (AIEE) (Figure1.2). [1,3,4]

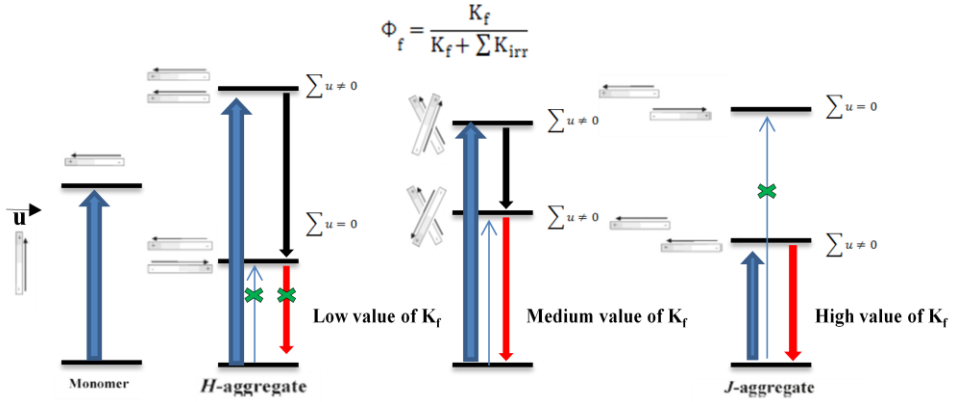

Figure 1.1. H- and J-aggregates and their impact on the absorption and emission processes in the framework of exciton models.

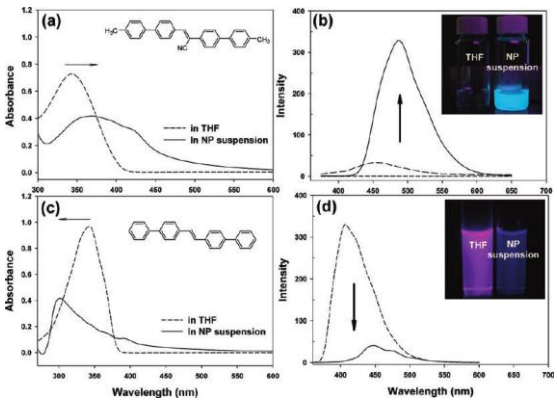

Figure 1.2. UV absorption and PL spectra of CN-MBE (a and b) and DPST (c and d) (2 x 10^{-5} M) in THF and NP suspensions (80 vol % water in THF), respectively. CN-MBE is J-aggregates and DPST is H-aggregates.

1.2 Piezochromism: Role of molecular packing in solid fluorescence of π-conjugated molecules

Molecular stacking in π-conjugated materials play a vital role in their optical properties, the ability to transport charge carrier, and supramolecular assembly[5,6,7]. Even if the chemical structure is identical, solid color and luminescence could be different from their molecular stacking. Piezochromism is the reversible luminescence or color changing phenomenon by mechanical stimuli. The induced color reverts to the original color by thermal stimuli, organic solvent vapor. The one of the mechanism, which is recently intensively studied for smart materials, is change of crystal structure by external stimuli.

For example, DBDCS[4(c)] was observed to "molecular sheets" assisted by multiple hydrogen bonds. Blue-crystal shows excitonic coupling. Grind force to Blue- phase promotes slip-stacking and increases excimeric coupling between DBDCS molecules. The driving force for the transition is provided by the local dipoles as introduced though the cyano group. The anti-parallel coupling of the cyano group kinetically makes the structures stabilize. Therefore, two-color luminescence switching stems from different slip-stack of molecular sheets. Like this, secondary interaction and local dipoles have a great influence on molecular stacking and mechanical stimuli responsive behavior companied with luminescence and crystal structure change. Awareness of the role of molecular packing in controlling solid-state optical properties of π-conjugated materials can be utilized for developing stimuli-responsive materials. [1]

1.3 Cis-Trans (E/Z) isomerization : Photochromism

Photochromism is simply defined a reversible transformation of a chemical species induced in one or both directions by absorption of electromagnetic radiation between two forms, A and B, having different absorption spectra (See Figure 1.3).[5.6] The thermodynamically stable form A is transformed into form B by irradiation.

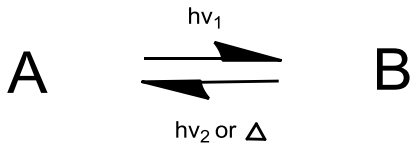

Figure 1.3 Photoisomerization of A and B

Cis-trans (E/Z)isomerization, which is one of families of organic photochromism, occurs in stilbenes, azo compounds, azines, and thioindigoids. The azobenzene and stilbene case is shown in Figure 1.4.

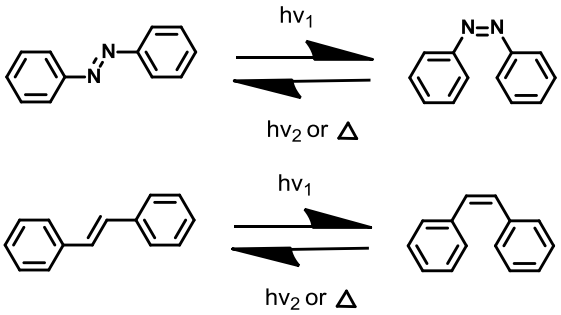

Figure.1.4 Photochromism in azobenzene and stilbene

Mechanisms of photoisomerization in azobenezene are explained by two models based on

inversion and rotation. In rotation mechanism, excitation by light would cleave the π-bond allowing rotation. Due to lone pair electron in nitrogen bonding in azobenzene, photoisomerization could occur by inversion without breaking π-bond. The cis form is not thermally stable with respect to the trans form, so the cis form reverts back to the trans form in the dark. Contrary to azo compounds, cis-stilbene is more stable that their azobenezenes counterparts. Also the barrier to thermal isomerization is significantly larger and the rate of thermal isomerization at room temperature is very slow. The main mechanism of photoisomerization is rotation since stilbene does not have lone pair electron in double bonding and n – π* transition.[5,6,7]

Cis-trans isomerization is controllable by temperature and special wavelength light. Normally, trans molecules shows larger absorption maximum wavelength and absorbance than cis molecules. Due to overlapped absorption spectra of two isomers with difference absorbance, photo stationary state (PSS) exists in each wavelength light. Based on PSS, the conversion ration of cis-trans transition is defined.

1.4 Research Objective

Crystal engineering is an important topic both in fundamental research field for the studies on crystal structure-property relationship and practical applications in developing self-assemble nanostructure. In organic π-conjugated molecules, the secondary intermolecular interactions play a vital role in determining packing motif arrangement, assemble structure and the related optoelctronic properties. For instance, our group reported a series of new cyanostilbene

derivatives exhibiting highly luminescence in the solid state such as powder, nanoparticle, gel, etc.[4,8]The optical behavior is attributed to the formation of specific supramolecular stacking architecture associated with the unique electronic and geometrical characteristics of the designed molecules. However, despite of the researches in crystal engineering, the role of intermolecular interaction to affect structure-properties relationship is uncertain. Therefore, the research is very significant issue to develop crystal engineering for not only the field of materials science but also application in high performance organic optoelectronic device.

Herein, I have studied structure-properties relationship of dicyanostyrylbenzene derivatives by comparing various length of alkoxy chain and cyano-group position. Firstly, I expored study on correlation between optical properties both in solution and solid state and α-,β-dicyanodistyrylbenzene. Also piezochromism and vaporchromism behaviors of the series of molecules were observed. Especially, I found novel phenomena which is sequential luminescence switching via mechanical and light stimuli. Furthermore, the change in time difference of fluorescence quenching by UV irradiation at mechanically perturbed state was observed as the function of length of alkyl chain and cyano group position, which means the phenomenon is strongly related with molecular assembly. Lastly, sequential multi-colored fluorescent switching via mechanical and light stimuli smart material is demonstrated.

I propose the mechanism for dramatical fluorescence quenching of DHDCS which is α-dicyanodistyrylbenzene with six-alkoxy chain. DHDCS shows piezochromism which is the change fluorescence color between green to yellow by shear force. Interestingly, the fluorescence quenching occurs rapidly at ground regions. DHDCS's isomers mixture were

separated by column purification from . The NMR analysis of isomers proves that fluorescence quenching mechanism is based on photoisomerization. However, the phenomena contradict the previously reported result which non-fluorescent cis-cyanostilbene in solid state tunes on luminescence by UV irradiation since highly fluorescence trans-cyanostilbene in solid state is generated and excited by energy transfer and emits light. Also even though DBDCS shows similar phenomena, the change in time difference of fluorescence quenching is very slow and over than that of DHDCS. I study photophysical properties such as UV/PL, fluorescence life time measurement and XRD of single crystal and powder. Thus, I successfully suggest the possible mechanism of the DHDCS unique piezo- and photo-chromism phenomena. Finally, I compared DHDCS single crystal and β-DBDCS, which is only analyzed among β-seires and do not show fluorescence quenching in perturbed film by UV stimuli, propose relationship between molecular packing and optical properties of piezo- and photo- dual chromism. These works will provide insight both into the field of crystal engineering research and the development in optical information application.

1.5 Bibliography

1. Shinto Varghese and Suresh Das, *J.Phys. Chem. Lett*. **2011**, 2, 863

2. Hong, Ym Lama, J.W.Y, Tang, B. Z, *Chem. Commun*. **2009**,4332

3. B.-K. An, J. Gierschner, S. Y. Park, *Acc. Chem. Res.* **2011**, *45*, 544

4. (a) B.-K. An, J. Gierschner, S. Y. Park, *Acc. Chem. Res.* **2011**, *45*, 544; (b) B.-K. An, S.-K. Kwon, S.-D. Jung, S. Y. Park, *J. Am. Chem. Soc.* **2002**, *124*, 14410. (c) S.-J. Yoon, J. W. Chung, J. Gierschner, K. S. Kim, M.-G. Choi, D. Kim, S. Y. Park, *J. Am. Chem. Soc.* **2010**, *132*, 13675; (d) S.-J. Yoon, J. H. Kim, K. S. Kim, J. W. Chung, B. Heinrich, F. Mathevet, P. Kim, B. Donnio, A.-J. Attias, D. Kim, S. Y. Park, *Adv. Funct. Mater.* **2012**, *22*, 61.(e) S.-K Park, J.H. Kim, S.J. Yoon, O.K. Kwon, B.-K An, S. Y. Park, *Chem. Mater*. **2012**, 24, 3263

5. H. Durr., H. Bouas-Laurent(Eds.)(Studies in Organic Chemistry 40), Elsevier, Amsterdam, 1990 (1068pp)

6. H. Bouas-Laurent,H. Durr., *Pure Appl. Chem*., **2001**, 73, 4, 639

7. H.M. Dhammika Bandara and S.C. Burdette., *Chem. Soc. Rev*., **2012**, 41, 1809

8. An, B.-K.; Lee, D.-S.; Lee, J.-S.; Park, Y.-S.;Song, H.-S.; Park, S.Y. *J. Am. Chem. Soc*. **2004**, 126, 10232

Chapter 2. Multiple Stimuli Responsive Piezochromic Materials Based on Dicyanodistyrylbenzene Molecules with Aggregation-Induced Enhanced Emission (AIEE): Studies on Piezochromic, Photoisomerization Behavior and Photophysical Property

2.1 Introduction

Solid-state luminescence switching materials to the environmental stimuli are attracting significant interest in view of their promising application in sensors, memories, and security inks. Among other stimulus, mechanical force responsive smart materials in molecular level are rare and not well developed. Especially, control of molecular phenomena by macroscopic mechanical stimuli is not well appreciated compared to covalent bonds cleave phenomena. For example, piezochromism of spiropyran to merocyanine conversion is clear and easily defined[1]. In contrast, some mechanical force such as shear force and compression may cause organic crystal deformation and ruptures but we do not understand detail what phenomena occur at the molecular level and why color or luminescence of piezochomic materials is changed. Awareness

of the role of molecular packing in controlling optical properties in solid state and crystal structure change by mechanical force can be utilized for developing stimuli-responsive smart materials[2].

To date, we have reported a novel class of asymmetric α-cyano-substitued stilbenic derivatives(CN-TrFMBE)[3] exhibiting unique and peculiar fluorescence behavior. Compared usually α-cyano-stilbene AIEE compound which is virtually non-fluorescent in solution but becomes highly fluorescent upon self-assembly into supramolecules[4], CN-TrFMBE shows shear- and UV-induced fluorescence switching. Interestingly, [2+2] cycloaddition by UV-irradiation induced intermolecular shear force causes fluorescence 'tune on' like piezochromic phenomena. Moreover, we have reported multiple stimuli responsive materials for dicyanodistyrylbenezen core, DBDCS. DBDCS exhibits blue to green fluorescence switching via vapor stimuli and mechanical stimuli. Our group successfully explains the fluorescence switching mechanism based on the correlation between optical properties and molecular stacking. Compelling hypotheses have been appreciated for each system. However it is not well studied in stimuli responsive behavior, optical properties and piezochromic phenomena relationship of smart materials. Also the molecular stacking change at molecule level accompanied with fluorescence change remains unclear.

Herein, I have reported eight piezochromic compounds. The molecules consist of rigid dicyanodistrylbenzene, which show bright solid-state fluorescence and piezochromism, with different lengths of alkoxy chain and position of cyano group. I study followings: i) the role of –CN group, ii) the role of length of alkoxy chain in piezochromism behavior, and iii) fluorescence switching by solvent vapor annealing stimuli. Interestingly, fluorescence quenching at mechanically perturbed state after UV irradiation was observed in α-

dicyanostrylbenzene derivatives. I proved that the phenomena are attributed to photo-isomerization by 1H NMR data and monitored and compared fluorescence quenching dynamics. In additionaly, I successfully demonstrated highly fluorescent and tri-colored patterns via piezo- and photo-chromism. Thererfore, I first report new class of smart materials which show very unique property by combining AIEE, piezochromism, and photoinduced isomerization behavior.

2.2 Experiments

2.2.1. Synthesis

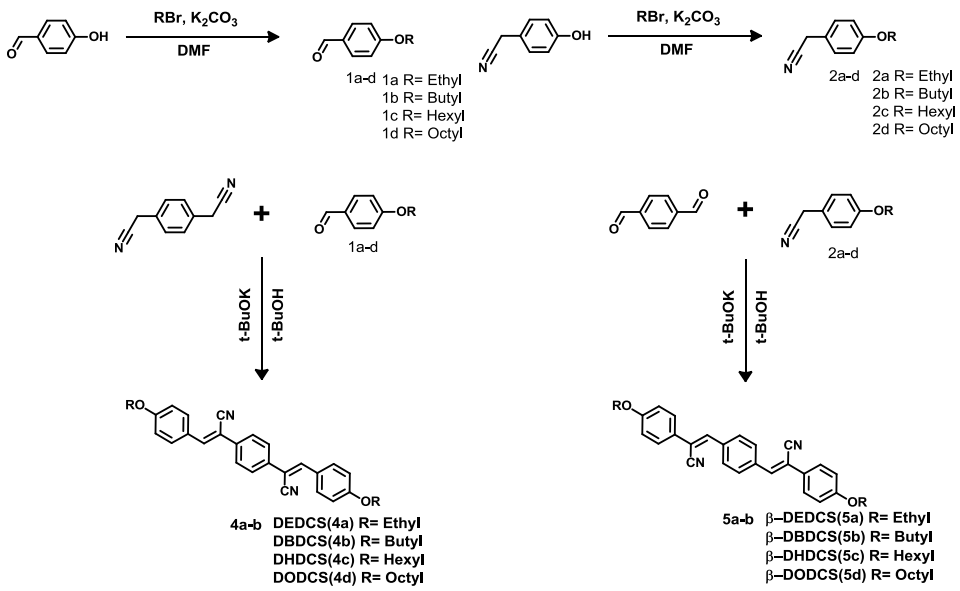

Scheme 2.1 Syntheic scheme of target molecules

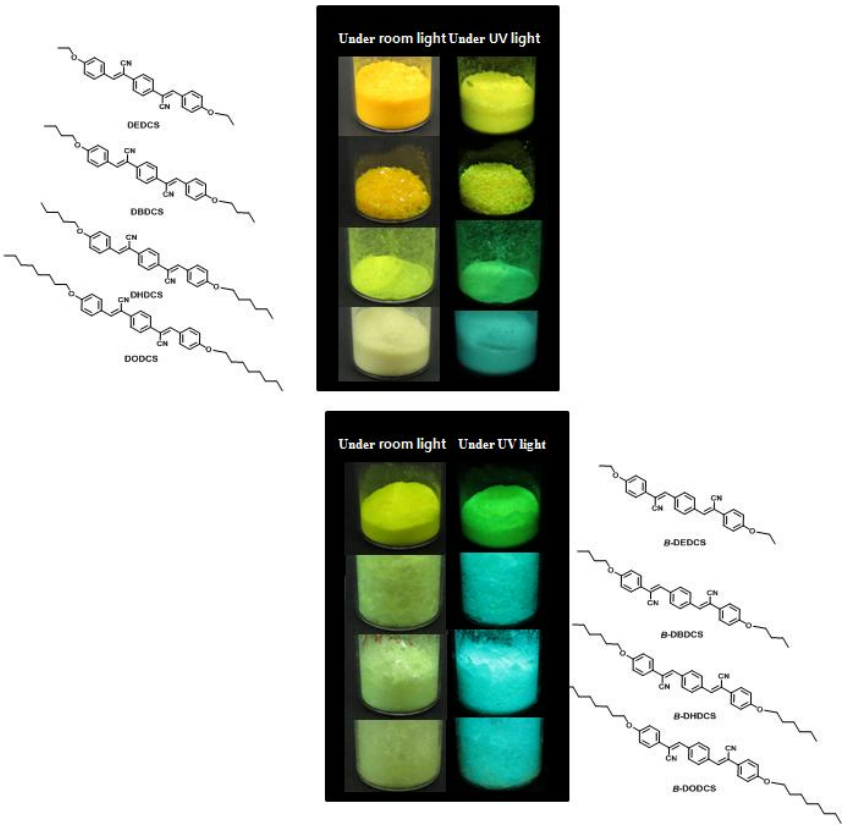

Figure 2.1 powder photo images of target materials

General Procedure for Alkylation of 4-hydroxyphenylaldehyde. (1a-1d)

A mixture of 4-hydroxyphenylaldehyde(3g,24.6mmol) and potassium carbonate(2.80g, 25.0mmol) in DMF was added 1-bromoalkane(25.0mmol) and stirred at 70^{o}C for 12 hour. After cooling to room temperature, the organic layer was extracted with dichloromethane and washed with brine. The organic phase was dried over $MgSO_4$, filtered and concentration in vacuo to give the crude product. The product was obtained by short colmn chromatography using ethyl acetate and n-hexane (1:5)

General Procedure for Alkylation of 4-hydroxyphenylacetonitrile. (2a-2d)

A mixture of 4-hydroxyphenylacetonitrile(3g,22.6mmol) and potassium carbonate(3.3g, 29.3mmol) in DMF was added 1-bromoalkane(29.3mmol) and stirred at 70^{o}C for 12 hour. After cooling to room temperature, the organic layer was extracted with dichloromethane and washed with brine. The organic phase was dried over $MgSO_4$, filtered and concentration in vacuo to give the crude product. The product was obtained by short colmn chromatography using ethyl acetate and n-hexane (1:5)

4-Ethoxyphenlyaldehyde (1a)

Yellowish liquid (3.32g, 90%) 1H.NMR (CDCl3) δ [ppm]: 9.88(s.1H,-CHO), 7.83(d.2H,Ar-H), 6.99 (d,2H,Ar-H), 4.12(q.,2H,OCH3), 1.45(t,3H,-CH3)

4-butoxyphenlyaldehyde (1b)

Yellowish liquid (4.16g, 95%) 1H.NMR (CDCl3) δ [ppm]: 9.88 (s, 1H, -CHO), 7.83 (d, 2H, Ar-H), 6.99 (d, 2H, Ar-H), 4.05 (t, 2H, -OCH2), 1.80 (m, 2H, -CH2), 1.51 (m, 2H, -CH2), 0.99 (t, 3H, -CH3).

4-Hexloxyphenlyaldehyde (1c)

Yellowish liquid (4.81g, 95%) 1H.NMR (CDCl3) δ [ppm]: Yellowish liquid (4.16g, 95%) 1H.NMR (CDCl3) δ [ppm]: 9.88 (s, 1H, -CHO), 7.83 (d, 2H, Ar-H), 6.99 (d, 2H, Ar-H), 4.05 (t,

2H, -OCH2), 1.80 (m, 2H, -CH2), 1.55-1.25(m, 6H, -CH2), 0.90 (t, 3H, -CH3).

4-Octyloxyphenlyaldehyde (1d)

Yellowish liquid (5.3g, 92%) 1H.NMR (CDCl3) δ [ppm]: 9.88 (s, 1H, -CHO), 7.83 (d, 2H, Ar-H), 6.99 (d, 2H, Ar-H), 4.05 (t, 2H, -OCH2), 1.80 (m, 2H, -CH2), 1.53-1.25(m, 10H, -CH2), 0.90 (t, 3H, -CH3).

4-Ethoxyphenlyacetonitrile (2a)

Yellowish liquid (3.31g, 90%) 1H.NMR (CDCl3) δ [ppm]: 7.23(d, 2H, Ar-H), 6.88(d, 2H, Ar-H), 4.02(q, 2H, -OCH2-), 3.67(s, 2H, NC-CH2), 1.43(t, 3H, -CH3)

4-butoxyphenlyacetonitrile (2b)

Yellowish liquid (3.80g, 89%) 1H.NMR (CDCl3) δ [ppm]: 7.21(d, 2H, Ar-H), 6.88(d, 2H, Ar-H), 3.95(t, 2H, -OCH2-), 3,67(s, 2H, NC-CH2), 1.76(m,2H, -CH2), 1.50(m, 2H, -CH2), 0.9(t, 3H, -CH3)

4-Hexloxyphenlyacetonitrile (2c)

Yellowish liquid (3.92g, 80%) 1H.NMR (CDCl3) δ [ppm]: 7.21(d, 2H, Ar-H), 6.88(d, 2H, Ar-H), 3.95(t, 2H, -OCH2-), 3,68(s, 2H, NC-CH2), 1.77(m,2H, -CH2), 1.45(m, 2H, -CH2), 1.32(m, 4H, -CH2), 0.9(t, 3H, -CH3)

4-Octyloxyphenlyacetonitrile (2d)

Yellowish liquid (4.32g, 78%) 1H.NMR (CDCl3) δ [ppm]: Yellowish liquid (3.92g, 80%) 1H.NMR (CDCl3) δ [ppm]: 7.21(d, 2H, Ar-H), 6.88(d, 2H, Ar-H), 3.95(t, 2H, -OCH2-), 3,68(s, 2H, NC-CH2), 1.77(m,2H, -CH2), 1.45(m, 2H, -CH2), 1.32(m, 8H, -CH2), 0.9(t, 3H, -CH3)

General procedure for Knovenagel condensation of 4a-4d

1,4-phenylenediacetonirile(1g, 6.4mmol) and 1a-1d(13.5mmol) was dissolved in t-BuOH(40ml) and THF(10ml). t-BuOK was slowly added into the mixture. After checking precipitate, the mixture was stirred for half hour. MeOH was poured into the mixture and the resulting precipitate was filtered. The filtrate was purified by column chromatography using dicholomethane. The final product was obtained by recrystallization from ethyl acetate.

(2Z,2'Z)-2,2'-(1,4-phenylene)bis(3-(4-ethlyoxyphenyl)acrylonitrile) (DEDCS,4a)

Yellowish crystalline powder(1.99g,74%) 1H.NMR (CDCl3) δ [ppm]: 7.90(d, 4H, Ar-H), 7.71(s, 4H, -Ar-H), 7.51(s, 2H, -C=C-H), 6.96(d, 4H, Ar-H), 4.10(q, 4H, -CH2), 1.46(t, 6H, -CH4)

(2Z,2'Z)-2,2'-(1,4-phenylene)bis(3-(4-butoxyphenyl)acrylonitrile) (DBDCS,4b)

Yellow crystalline powder(1.98,65%) 1H.NMR (CDCl3) δ [ppm]: 7.90(d, 4H, Ar-H), 7.71(s, 4H, -Ar-H), 7.51(s, 2H, -C=C-H), 6.98(d, 4H, Ar-H), 4.04(t, 4H, -CH2), 1.81(m, 4H, -CH2), 1.51(m, 4H, -CH2), 0.99(t, 6H, -CH3)

(2Z,2'Z)-2,2'-(1,4-phenylene)bis(3-(4-hexyloxyphenyl)acrylonitrile) (DHDCS,4b)

Green crystalline powder(2.72g, 80%) 1H.NMR (CDCl3) δ [ppm]: 7.90(d, 4H, Ar-H), 7.71(s, 4H, -Ar-H), 7.51(s, 2H, -C=C-H), 6.98(d, 4H, Ar-H), 4.03(t, 4H, -CH2), 1.81(m, 4H, -CH2), 1.51(m, 4H, -CH2), 1.36(m,8H,-CH2), 0.99(t, 6H, -CH3)

(2Z,2'Z)-2,2'-(1,4-phenylene)bis(3-(4-octyloxyphenyl)acrylonitrile) (DODCS,4b)

Pale yellow crystalline powder(3.42g, 91%) 1H.NMR (CDCl3) δ [ppm]: 7.90(d, 4H, Ar-H), 7.71(s, 4H, -Ar-H), 7.51(s, 2H, -C=C-H), 6.98(d, 4H, Ar-H), 4.03(t, 4H, -CH2), 1.81(m, 4H, -CH2), 1.48(m, 4H, -CH2), 1.35(m, 8H,-CH2), 0.91(t, 6H, -CH3)

General procedure for Knovenagel condensation of 5a-5d

Terephthaldehyde(0.8g, 6.0mmol) and 2a-2d(13.0mmol) was dissolved in t-BuOH(40ml). t-BuOK was slowly added into the mixture. After checking precipitate, the mixture was stirred for half hour. MeOH was poured into the mixture and the resulting precipitate was filtered. The filtrate was purified by column chromatography using dicholomethane. The final product was obtained by recrystallization from ethyl acetate.

(2Z,2'Z)-3,3'-(1,4-phenylene)bis(2-(4-ethoxyphenyl)acrylonitrile) (β-DEDCS,5a)

Green crystalline powder (2.03,81%) 1H.NMR (CDCl3) δ [ppm]: 7.95(s, 4H,Ar-H), 7.63(d, 4H, Ar-H), 7.42(s, 2H, -C=C-H), 6.96(d, 4H, Ar-H), 4.10(q, 4H, -OCH2), 1.45(t, 6H, -CH3)

(2Z,2'Z)-3,3'-(1,4-phenylene)bis(2-(4-butoxyphenyl)acrylonitrile) (β-DBDCS,5b)

Cyane bulk powder **(1.90g, 67%)** 1H.NMR (CDCl3) δ [ppm]: 7.95(s, 4H,Ar-H), 7.63(d, 4H, Ar-H), 7.42(s, 2H, -C=C-H), 6.96(d, 4H, Ar-H), 4.10(t, 4H,-OCH2), 1.80(m,4H , -CH2), 1.55-1.47(m, 4H, -CH2), 0.99(t, 6H, -CH3)

(2Z,2'Z)-3,3'-(1,4-phenylene)bis(2-(4-hexyloxyphenyl)acrylonitrile) (β-DHDCS,5c)

Cyane bulk powder (2.35g, 74%) 1H.NMR (CDCl3) δ [ppm]: 7.95(s, 4H,Ar-H), 7.61(d, 4H, Ar-H), 7.42(s, 2H, -C=C-H), 6.96(d, 4H, Ar-H), 4.00(t, 4H,-OCH2), 1.80(m,4H , -CH2), 1.47(m, 4H, -CH2), 1.35(m, 8H, -CH2), 0.92(t, 6H, -CH3)

(2Z,2'Z)-3,3'-(1,4-phenylene)bis(2-(4-octyloxyphenyl)acrylonitrile) (β-DODCS,5d)

Cyane bulk powder (2.70g, 77%) 1H.NMR (CDCl3) δ [ppm]: 7.95(s, 4H,Ar-H), 7.62(d, 4H, Ar-H), 7.42(s, 2H, -C=C-H), 6.96(d, 4H, Ar-H), 4.00(t, 4H,-OCH2), 1.82(m, 4H , -CH2), 1.31(m, 20H, -CH2), 0.88(t, 6H, -CH3)

2.2.1 Spectroscopic Characterization.

^{1}H-NMR spectrum was recorded on a Bruker, Avance-300 (300 MHz) in $CDCl_3$ Solution. ^{1}C-NMR was recorded on a Bruker, Avance-500 (500 MHz) in $CDCl_3$ Solution. Mass spectra were recored on JEOL. JMS-700 spectrometer using fast atom bombardment (FAB) method.

Significant fragments are reported in the following fashion: m/z (relative intensity). Elemental analysis was carried out using a CE instruments, EA1110 elemental analyzer. UV-visible absorption spectra were recorded on Shimazu, UV- 1650 PC spectrometer. Photoluminescence spectra were obtained using a Photo Technology International, Felix32 QM-4 and a Varian, Cary Eclipse Fluorescence spectrophotometer. The relative fluorescence quantum yield was measured using quinine sulfate in 1.0N H_2SO_4 as a standard reference ($1x10^{-5}$ mol L^{-1}, $\boldsymbol{\Phi}_F$=53.5%). The absolute $\boldsymbol{\Phi}_F$ values of powder and thin films on quartz plates were measured using a Photo Technology International, Felix32 QM-4 with a 3.5 inch integrating sphere. Time-resolved fluorescence lifetime experiments were performed by the time-correlated single photon counting (TCSPC) technique with a FluoTime200 spectrometer (PicoQuant) equipped with a PicoHarp300 TCSPC board(PicoQuant) and a PMA182 photomuliplier(PicoQuant). The excitation source was a 377nm picoseconds pulsed diode laser (PicoQuant, LDH375) driven by a PDL800-D driver (PicoQuant) with fwhm ~ 70 ps. The muli-exponetial least square fitting procedure was carried out with the Fluofit software (PicoQuant), taking into possible double excitations of the IRF within the deconvolution. Mean decay times τ_{av} were obtained from the individual lifetimes τ_i and amplitudes α_i of muli-exponentail evaluation through

$$\tau_{av} = \frac{\sum_i \alpha_i \tau_i^2}{\sum_i \alpha_i \tau_i}$$

2.2.2 Thermal Analysis.

The thermal properties were investigated using a differential scanning calorimetry (DSC) with TA Instruments and DSC-Q1000 instruments operated at a heating rate of 10 ℃ min^{-1}.

2.3 Result and discussion

2.2.1 Design concept and target materials

While our group suggest that piezochromism mechanism of DBDCS, we did not explain the general rule of piezochromism or stimuli responsive behavior based on molecular assembly. To explore fluorescence change behavior with molecular assembly, we fixed chromphore core and modified moelcule structureby changing the length of alkoxy chain. First, we syntheized DBDCS derivatives with various length of alkoxy chain in order to tune molecular assembly finely. Also, β-cyanostilbene derivatives, which were reported by Weder groups for optical application such as piezochromism and optical storage[5], were made in order to understand the role of cyano group position in controlling molecular stacking and in stimuli responsive behavior.

In my research, I focused on photoluminescence properties in solid state of DCS derivatives. Futhermore, I studied relationship between piezochromism and various molecule structure; alkoxy chain length and cyano group position. In order to clearly understand the relationship with optical properties and molecule structure in solid state, I study following i) the role of alkoxy chain length and –CN location to influence photoluminescence in solid state ii) photophysical properties changes by mechanical and solvent vapor stimulis iii) understanding the origin of unique phenomena, luminescence quenching at mechanical perturbed state. Now, I discuss photoluminescence, piezochromic behavior and optical properties of the target

materials(See Figure 2.1).

2.2.2 Optical property

Optical properties of eight DCS derivatives in solution and in nanoparticles were investigated. Bacially, each α-,β- series show the same UV and PL spectra in solution state because their π-conjugated backbone which determins intrinsic optical property is identical(Figure 2.2 and 2.3). Absorption spectra of β-series in solution exhibit bathochromic shift against α-series. This indicates that β-series π-orbital in molecules‘ backbond is more delocalized and conjugated. This explanation concides the result of photoluminescence data. β-series show highly fluorescence(Φ_{QY}~0.4) in solution state but α-series present no fluoresecence(Φ_{QY}<0.0001). Due to less conjugated backbond of α-series, non-radiative decay by rotation process of α-series in solution might be strongly activatied. Therefore α-series do not exhibit fluorescence.

In absorption spectra, the maximum of the nanoparticles of all target materials are hyporchrmoic shifted againt solution(Figure 2.4). The spectra changes are attributed to H-type aggregtion which usually cause fluorescence quenching in solid state[6]. However, both series show strong fluorescence emission in nanoparticle. β-series have intrinsically strong fluorescence property and thus it is not surprised nanoparticles of the molecules exhibit strong fluorescence. α-series show aggregation-induced enhanced emission (AIEE) behavior even though the aggregation characteristic are H-aggregation. In aggregation state, non-radiative decay by rotation of α-series is surpressed. We can observe a red-shifted shoulder peak in nanoparticles‘ absorption spectra which means that S0 ->S1 transition is not dipole-moment forbidden transition even in H-type aggregation. S1->S0 transition is allowed and fluorescene

K_f value is enough value for fluorescence. Therefore α-series present high $\Phi_{FL}[= K_f/(K_f+\sum K_{irr})]$ and emit strong light in H-aggregated nanoparticle

The role of alkoxy chain length is quite complicated. In α-series, there are no inclination about length of alkoxy chain. Nanoparticles of DEDCS and DODCS emit yellow emission(λ_{max}~560nm) under UV illumination. Fluorescence quantum yield and brightness of DEDCS and DODCS are quit low. DBDCS and DHDCS exhibit similar fluorescence quantum yield and green emission(λ_{max} ~530nm). In β-series, all molecules emit cyan fluorescence (λ_{max} ~500-520nm in nanoparticles). In particular, absorption spectra are the almost same except for β-DEDCS. In the optical properties data, we could know that the alkoxy chain length have a great influenece on molecular stacking of α-series but we could not know exactly how to modify molecular packing. Also we guess that molecular assembly of β-series is identical even though their molecular sturctures are different according to the lengthh of alkoxy chain. The photophysical properties of the series of molecules are summarized in Table 2.1

We could conclude that the alkoxy chain length and cyano group location in molecules play a vital role in molecular stacking and photophysical properties in solid state. Even though single crystal analylsis are need to clearly understand molecular stacking, the optical data gives a insight to the role of alkoxy chain and cyano group for molecular packing in solid state.

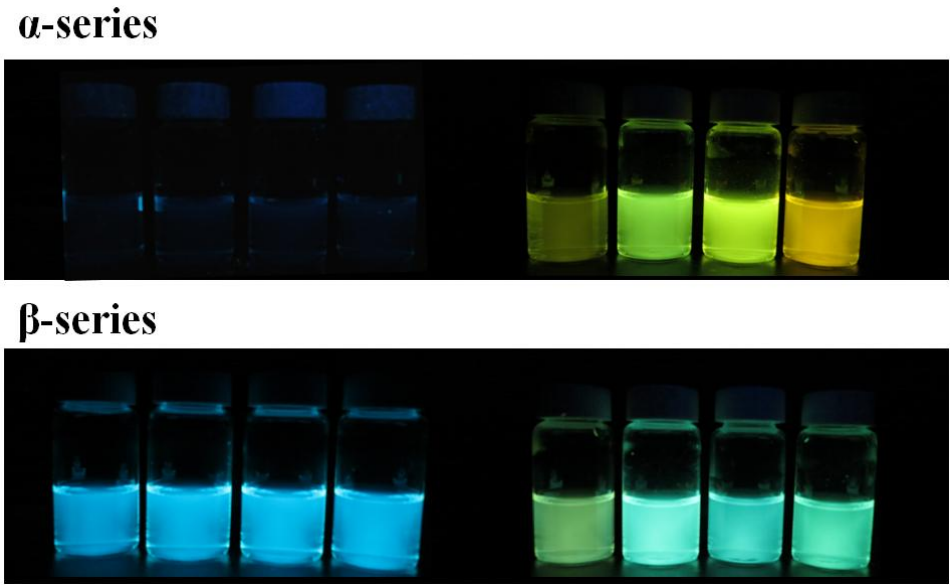

Figure 2.2 Photo of solution and nanoparticles suspension of α-series and β-Series under UV illumination. Alkoxy chain length increase from left side to right side(From two to eight).

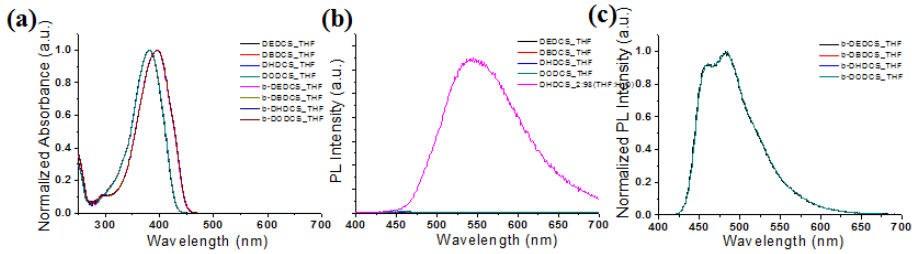

Figure 2.3 (a) Normalized absorption Spectra of the series molecules in solution (b) PL spectra of α-series in solution and DHDCS nanoparticles. Compared to DHDCS nanoparticle PL, α-series show no fluoresence. (c) PL spectra of β-series in solution

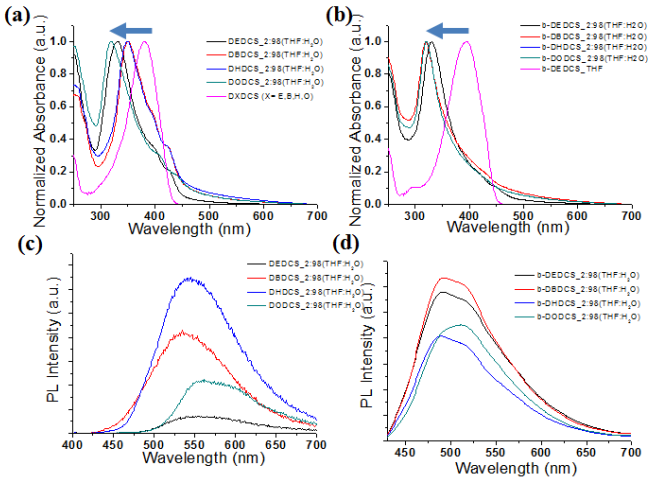

Figure 2.4 (a) Normalized Absorbance spectra of α-Series in nanoparticle suspension (b) Normalized Absorbance spectra of β-Series in nanoparticle suspension (c) PL spectra of α-Series in nanoparticle suspension (d) PL spectra of β-Series in nanoparticle suspension

Molecules	λ^{max}_{abs} [nm][(a)]	λ^{max}_{abs} [nm][(b)]	λ^{max}_{em} [nm][(a)]	λ^{max}_{em} [nm][(b)]	Φ_f[%][(a)]	Φ_f[%][(b)]
DEDCS	380	331	n.d[(c)]	548	0[(d)]	26
DBDCS	380	350	n.d[(c)]	535	0[(d)]	29
DHDCS	380	349	n.d[(c)]	544	0[(d)]	32
DODCS	380	318	n.d[(c)]	554	0[(d)]	29
β-DEDCS	395	330	483	493	4	16
β-DBDCS	395	319	483	491	9	22
β-DHDCS	395	319	483	488	19	15
β-DODCS	395	319	483	515	15	14

(a)Solution (b) Nanoparticle Suspension (c) Non-determinated (d) <0.01%

Table 2.1 Photophysical Properties of the series molecules in THF solution (c = 2 x 10^{-5} mol L^{-1}) and nanoparticles in (2%)THF/water mixture (c = 2 x 10^{-5} mol L^{-1}). Excitation wavelength is 360nm. The relative quantum yield is measured by unsing quinine sulfate in 1.0 N H_2SO_4(aq) solution as a standard reference (1 x 10 10^{-5} mol L^{-1}, Φ_{PL}=0.545).

2.2.3 Fluorescence switching by mechanical and solvent vapor stimulis

As shown in Figure 2.5-Figure 2.8, all of the target materials show fluorescence switching via mechanical stimuli and solvent vapor stimuli in doped PMMA film and/or solid powder. It is known that the color switching phenomena stems from molecular stacking changes. Mechanical stimuli can cause the stacking change in one of two ways. Firstly, crystal to amorphous state transition is common in piezochromism mechanism. By grinding, crystalline structure is disturbed and we can observe that powder XRD peaks are broadened or disappeared and halo is appeared. DBDCS is one of the most famous materials showing crystal-to crystal transition mechanism. In this case, new XRD peaks could be observed when powder is ground. Eventually, the alternation of molecule stacking enviorments leads to change of transition dipole moment interaction and color. As already reported by our group, solvent vapor stimuli or solvent vapor annealing (SVA) cause nanoparticle aggregation or nanoparticle size growth in doped PMMA film[7]. Unlike aggregation mechaism, SVA results in variation of molecular stacking and optical properties of alkoxy end substitued α-, β- dicyanodistilbenzene. Unfortunally, I could not obtain SVA annealed single crystal in order to XRD analysis and study SVA annealing effect deeply. However, photophysical property study will gives a insight to the role of SVA in crystal structure change.

2.2.3.1 Piezhochromism

Piezhochromism is defined that color or fluorescence of materials switching via mechiancal force and the origianl color of fluorescence is recovered in the dark or by heat. Due to polymorphism of dicyanodistyrylbenzene, I had to select the starting state which could restore by stimuli after grinding. In this view, DEDCS shows tribochromism which is irreversibly color change by mechanical force but not piezhochromism. DEDCS's fluorescence color or fluorescence intensity is altered when the powder and doped PMMA film is grinded. However, the starting color could not be restored even if the samples were annealed. If annealed temperature increases, the sample is melted. As already reported by our group, DBDCS shows reversible fluorescence switching. Blue color(λ_{max}=458nm), which is monomeric emission, is converted to unstructured excimer green fluorescence emission (λ_{max}=538nm) by shear force in DBDCS. DHDCS show green(λ_{max}=530nm) to yellow(λ_{max}=551) fluorescence switching by mechanical force. The green color is recovered after heating. DODCS recrystallized from EA exhibits pale cyanine (λ_{max}=498 nm) fluorescence crystalline powder. Unlike other α-series, the cyanine fluoresecnce of powder could not be obtained in doped PMMA film. As casted DODCS-doped PMMA film shows bright green emission. After annealed, the film is transparent. The fluorescence of film is pale green. By shear force, the pale green is converted to yellow(λ_{max}=549nm). The color switching is also reversible when it is heating.

Previously, Weder already reported β-dicyanodistilbene doped polymers which show piezochromic behavior when the polymer is streched. The mechanism of piezhochromism is excimeric and monomeric emission switching via aggregation and de-aggregation state. The

tensile force could adjust density of dyes in polymer matrix and aggregation[5a]. In this work, I fabricated doped polymer film by different methods; spin-casting. Also shear force rather than tensile force was applied as stimuli. β-DEDCS shows piezochromic behavior in powder. Fluorescence of prisitin powder(λ_{max}=498nm) is similar to that of solution((λ_{max}=483). After grinding, the color is changed to yellow(λ_{max}=575nm). Weder group reported previously that β-DEDCS emited cyan-blue as monomeric emission in de-aggregation state and green as excimeric emission in aggregation state. We can expect that cyan-blue powder shows weak excimeric coupling and emits structured emission spectrum under UV irradiation like DBDCS Blue phase. In ground yellow powder, eximeric couplng substantially increases and eximer emission is evloved. The fluorescence switching, however, could not be observed in doped PMMA film. This is becasue that β-series is poor soluble in any kind of solvents. During the film preperation, I tried to make highly doped thick and uniform PMMA film as possible but the concentration in saturated THF solution is only 0.4~0.6wt%. during the experiment, we found that piezochromic behavior in low concentrated PMMA film is not easy to be observed in both α-, β- dicyanodistilbenzen. Therefore low concentrated β-DEDCS film does not show any piezochromism. β-DBDCS, β-DHDCS and β-DODCS exhibit the similar piezochromic behavior in powder. Three powder sample's PL spectra are the almost same. Like β-DEDCS, the pristine powders' cyan-blue fluorescence(λ_{max}=460~475nm) change to yellow((λ_{max}=560~575nm) by shear force. Due to low solubility, the fluorescence switching of in doped PMMA film is similar to that of powder but is incomplete conversion. The series materials' piezochromism is summarized in Figure 2.5~ Figure 2.8 and Table 2.2.

2.2.3.2 Vaporchromism and Piezhochromism

Vaporchromism is phenomena which is accompanying color change by solvent vapor. Vaporchromism is well researched in organometallc and coordination complex for chemical vapor or solvent sensor[8]. In Pt-complex case, solvent vapor can diffuses metal complex crystal lattice. The vapor molecules interact metal-complex dipole or hinder metal-complex interaction which causes to vaporchromism. Also, in piezochromism, it is well known that solvent vapor leads to recover the original color from the induced color by mechanical force like thermal annealing. Our group reported two type vaporchromism. First example reported vapor induced deaggregation, controlling AIEE behavior. The Other one is that amorphous to crystal transition by solvent vapor evolves AIEE behavior. Compared to the vaporchromisms, α-, β-dicyanodistilbenzen show different vaporchromic behavior. Solvent vapor causes crystal to crystal transition and luminescent color changes. Interestingly, vapor and thermal stimuli make different results in fluorescence switching aganist conventional piezochromic materials.

To confirm SVA effect, I carried out experiment in dye-doped PMMA films. DEDCS's color change via dichloromethane(MC) vapor was observed; the fluorescence intensity increases and the absorption band is red-shifted. Normally, when slip angle increases, J-type stacking feature is strengthened and the absorption shape is bathchromic shift. It could be expected that Vaporchromic color is brighter than the original due to improve J-aggregation character. In vapor annealed state, DEDCS presents tribochromic behavior. The original color(λ_{max}=541) is converted to red-shifted color(λ_{max}=557). The original color and absorption spectra could not restored by any stimuli. Upon exposing at DBDCS film to MC vapor, the color of film becomes

green(λ_{max}=525). The green is different from the color of ground DBDCS powder and film. We found that SVA film of DBDCS also show piezochromism. The fluorescence color is altered from green to yellowish green(λ_{max}=538) when shear force was applied. If ground SVA film is annealed by vapor, the original SVA film color is recovered. After thermal annealing, blue color is returned. Therefore, DBDCS could control fluorescence color by SVA, piezowriting and thermal heating. In absorption spectum, SVA has effect on red-shift which means that solvent vapor induced sheet slip of the molecules. In DHDCS case, vaporchromism was not observed. Even thought the color of pristine film and vapor treated film look like slight different green, the absorption and PL spectra are the same both in as-casted film and vapor treated film. By vapor annealing, the fluorescence of DODCS is dramatically quenched. The maximum wavelength of absorption is blue-shifted after vapor treatment. Based on fluorescence quenching and blue-shifted absorption, I deduced that the slip angle decreases and DODCS dimer exhibit perfectly H-type aggregation. By shear force, SVA treated DODCS film shows red-shift absorption peak (from 300nm to 352nm) and fluorescence turn-on(λ_{max}=552nm). Vapor treated DODCS crystal might be slipped by shear force and restore J-type feature. Therefore the ground sample presents fluorescence. DODCS shows piezochromism due to restoration by vapor treatment. However, SVA sample could not return preannealed film's color by thermal annealing. If annealing temperature increases, DODCS phase become liguid crystal phase(LC) and PMMA doped film is dewetted.

β-Series have similiar vaporchromsim and piezochromism under SVA film. In spectrum, PL shapes are broader toward short wavelength region. Also PL intensity decreases. Due to a low concentration film, the absorbance of film is too small to classify maximum wavelength of each state. I guess the two possilbe vaporchromic effect on β-Series. First, solvent vapor plays a role

in aggregation of dispersed dyes. Hence, the emission intenstiy increases without changes in PL shapes. Second, SVA influences crystal structure to improve H-type feature. Therefore, red-shifted shoulder peak in absorption spectra is disappeared after vapor annealing. After grinding, fluorescence intensity increases and maximun wavelenth of both absorption and emission spectra is red-shifted. This might be because slip-angle increases by mechanical force and J-type charater improves. All β-Series show reversible piezochromism and vaporchromism. The whole phenomenon is summarized in Figure 2.5- 2.8 and Table 2.2

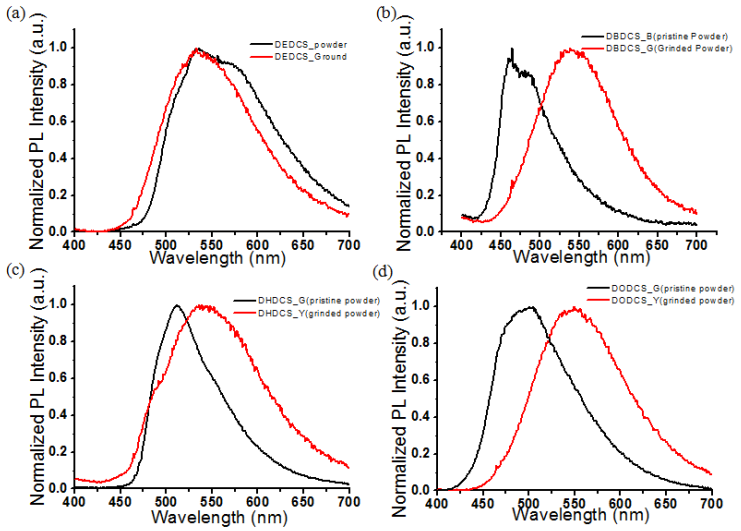

Figure 2.5 PL spectra of α-series pristine powder and ground powder. (a) DEDC, (b) DBDCS, (c) DHDCS ,(d) DODCS

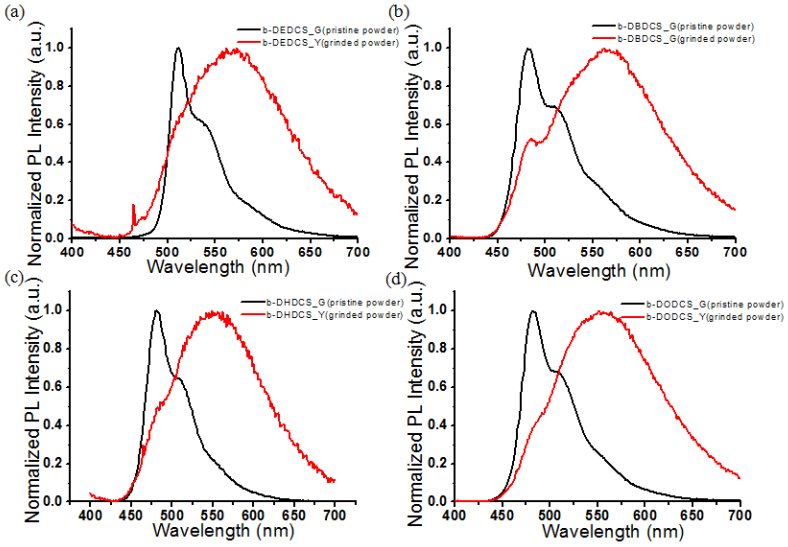

Figure 2.6 PL spectra of α-series pristine powder and ground powder. (a) β-DEDC, (b) β-DBDCS, (c) β-DHDCS ,(d) β-DODCS

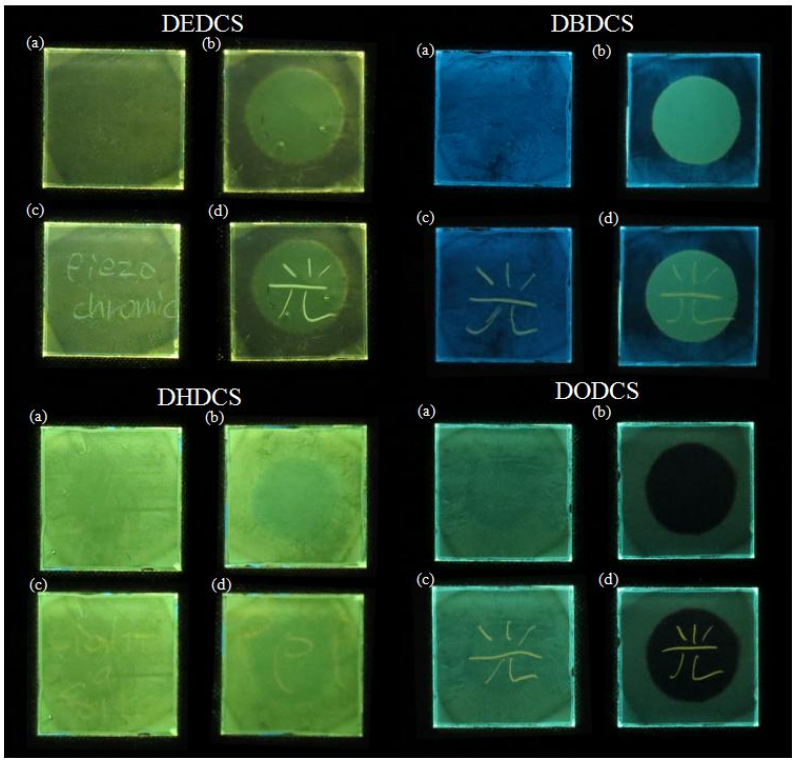

Figure 2.7 Photo of α-series doped PMMA film. (a) as-casted or pre-annealed film .(b) solvnet vapor annealed film. (c) ground film from (a). (d) ground film from (b)

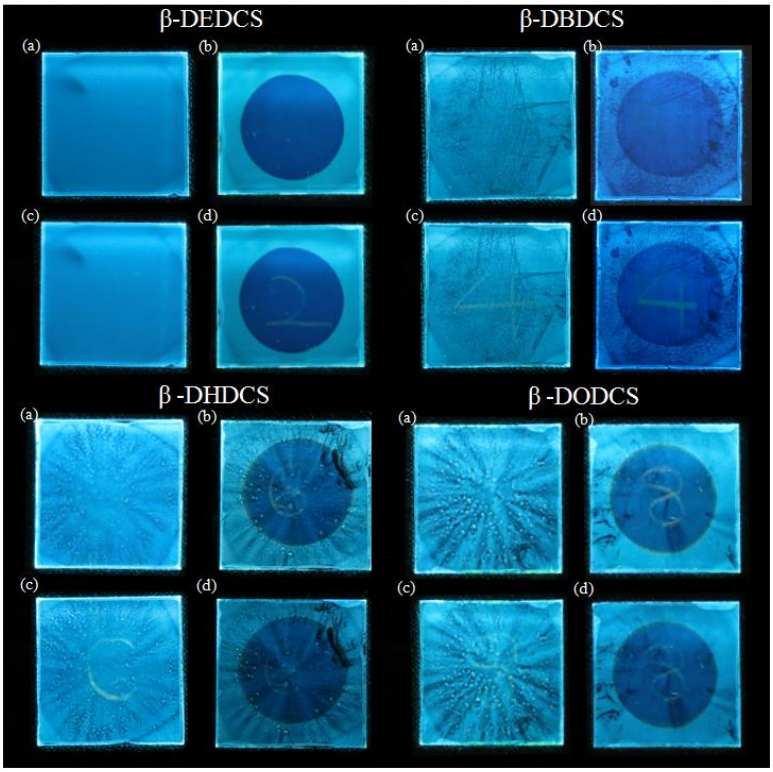

Figure 2.8 Photo of β-series doped PMMA film. (a) as-casted or pre-annealed film .(b) solvnet vapor annealed film. (c) ground film from (a). (d) ground film from (b)

Molecules	λ^{max}_{em} Unground[nm][a]	λ^{max}_{em} Ground[nm][a]	λ^{max}_{em} annealed[nm][a]	λ^{max}_{em} SVA[nm][a]	λ^{max}_{em} SVA-grounded[nm][a]	λ^{max}_{em} re-SVA[nm][a]
DEDCS	549	539	X[b]	541	557	X[b]
DBDCS	458	538	458	525	538	520
DHDCS	530	551	535	530	551	532
DODCS	513	549	512	n.d[c]	552	n.d[c]
β-DEDCS	498	X[d]	X[d]	487	571	492
β-DBDCS	483	483,559	483	483	483,568	483
β-DHDCS	489	489,552	489	477	489,551	487
β-DODCS	490	490,529	490	490	490,529	529

(a) Doped PMMA film (b) no change, irreverible process (c) non derterminated (d) no change

Table 2.2 Summary of piezochromism and vaporchromism of the target molecules**.**

2.2.5 Photoisomerization

Stilbene or azobenzen is well known that trans-cis or cis-trans photoisomerization occurs under UV irradiation. The phenomena can be observed in solution or amorphous state like polymer film. In crystal solid, photoisomerization is not usually allowed because free volume for isomerization is limited. In special case, solid soft materials show photoisomerization depending on the temperature. I observed the unique phenomena, quenching at mechanical perturbed state under UV irradiation. As far as I know, this phenomena is the first reported one among piezochromic materials. Herein, I elucidated origin of the fluorescence quenching related to photoisomerization.

As seen in Figure 2.9 and 2.10, fluorescecnce of piezo-writing regions in several sample is quenching under UV irradiation. To understand the main reason, we study about photophysical properties and NMR analysis of DHDCS. In THF solution, photoisomerzation occurs under UV irradiation. Short wavelength shoulder peak was appeared and increased when the same was irradiated(Figure 2.11). The change was already reported to photoisomerization of cyanostilbene[9]. I found that Photo-stationary state(PSS) was reached in 400s. By comparing abosption spectrum fluorescecne quenched film of DHDCS by UV irradiation, unstructured absorption shape in solid state is similar with that of solution. Also, maximun wavelength of absorption in the film is similar to that of shoulder peak of isomer mixture of DHDCS in solution. In NMR anaylsis, each peak of DHDCS solution irradiated by UV is fully matched with DHDCS ground powder under UV irradition(Figure 2.12). In absorption spectrum of the solution, the presence of isobestic point at 300nm implies that any kind of photochemical side

reaction so called photobeaching could be excluded during the measured irradiation time range (within ~400s). I conclude that Photoisomerzation cause to fluorescence quenching at mechanically perturbed state.

As shown in Figure 2.9, most of α-series doped films show sequential piezochromism and photochromism. However, time for fluorescence quenching under UV irradiation is different from molecules and/or polymorphism. For example, mechancial sheared region of DHDCS shows fluorescence quenching about 90s. In DBDCS blue phase case, green color in piezo-writing was disappered by UV over 12min. Thermal preannealed and solvent vapor annealed DODCS doped PMMA film samples show different phenomenon by mechincal and UV stimuli. Photoisomerization and fluorescence quenched occurs in the former sample after grinding. In constrast, the fluorescence quencing in the latter was not observed during 15min irradiation. Fluorescence intensity in smear region decreased but was not quenched after 2 hour irradiation. Also fluorescnce of other side region which is not treated by solvent vapor was dimed. It is considered that the color change by long time irradiation is not photoisomerization but is closed to photobleaching. Therefore, thermal preannealed film of DODCS shows sequntial piezo- and photo- chromism but SVA DODCS presents only piezochromism. The results indicate that dual action piezo- and photo-chromism stem from molecular assembly but does not intrinsic molecule properties. Compared to α-Series, β-Series exhibit only piezochromism. Like SVA DODCS, fluorescene in smear region beaome dimmer but was not disappeared after 2 hour UV irradiation. To clearly understand why photoisomerzation occurs in some samples or special state and clarify the detailed mechanism, I had to further study it. In chapter 3, I proposed the sequntial piezo- and photo-chromisc mechanism with several data analysis. I summarized the dual action phenomenon in UV/PL spectra from Figure 2.14 to Figure 2.20

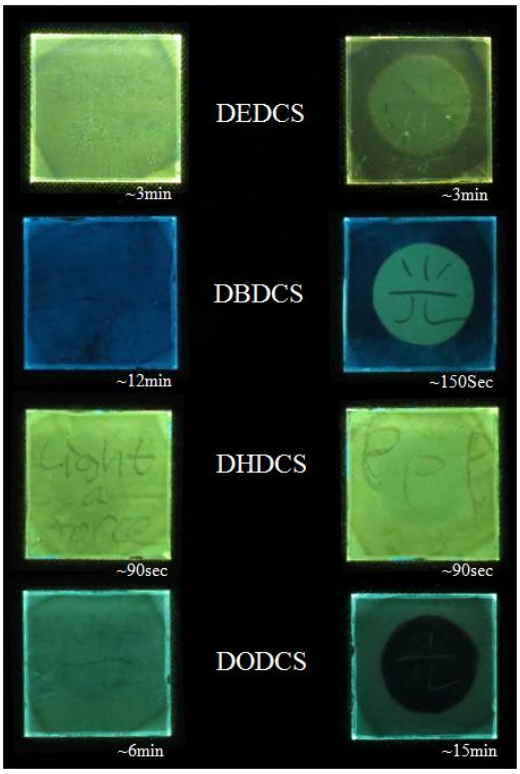

Figure 2.9 Photo of UV irradiated film in time difference. α-series molecules doped PMMA film. Left side shows as-casted or preannealed film. Right side shows is solvent vapor annealed film.

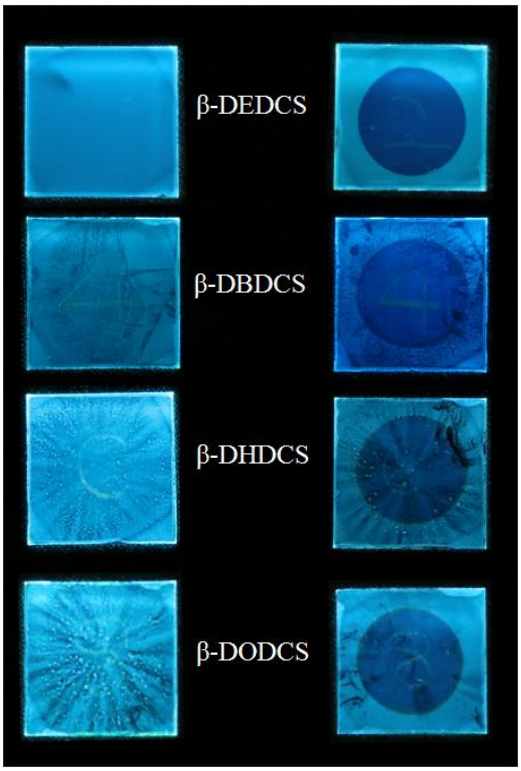

Figure 2.10 Photo of UV irradiated film in time difference. β-series molecules doped PMMA film. Left side shows as-casted or preannealed film. Right side shows is solvent vapor annealed film.

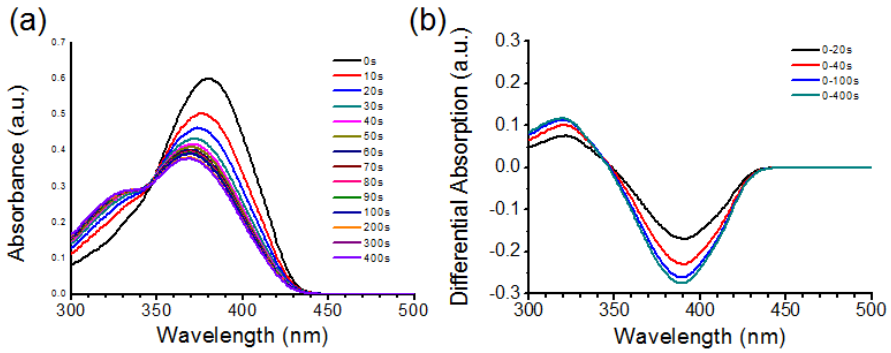

Figure 2.11 Absorption spectra of (Z,Z)-DHDCS solution in THF (2x 10^{-5} M) depending on UV irradiation time.

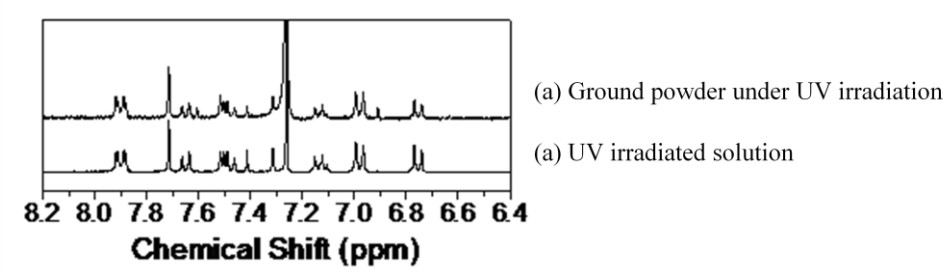

Figure 2.12 ^{1}H-NMR of Ground podwer under UV irradiation and UV irradiated solution of DHDCS.

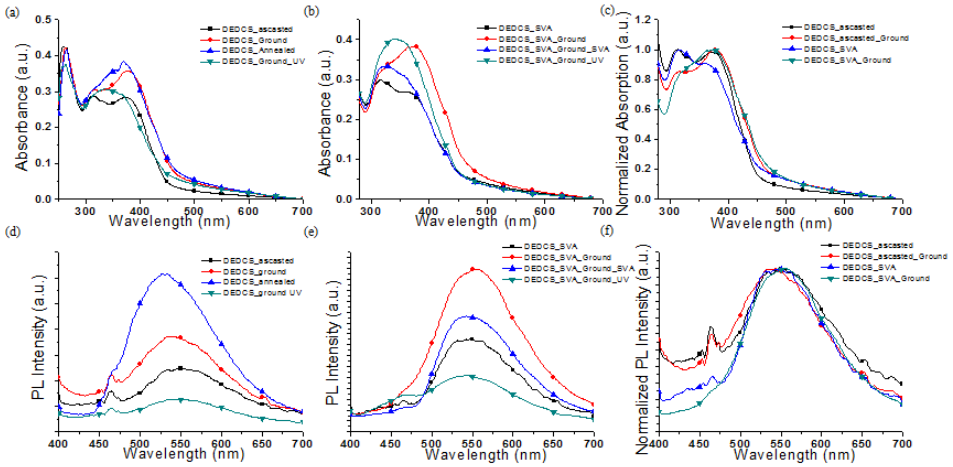

Figure 2.13 UV/PL spectra of DEDCS doped PMMA film. (a),(b),(c) UV absorption and normalized absorption spectrum of the film (d),(e),(f) PL and Normalized PL spectrum of the film.

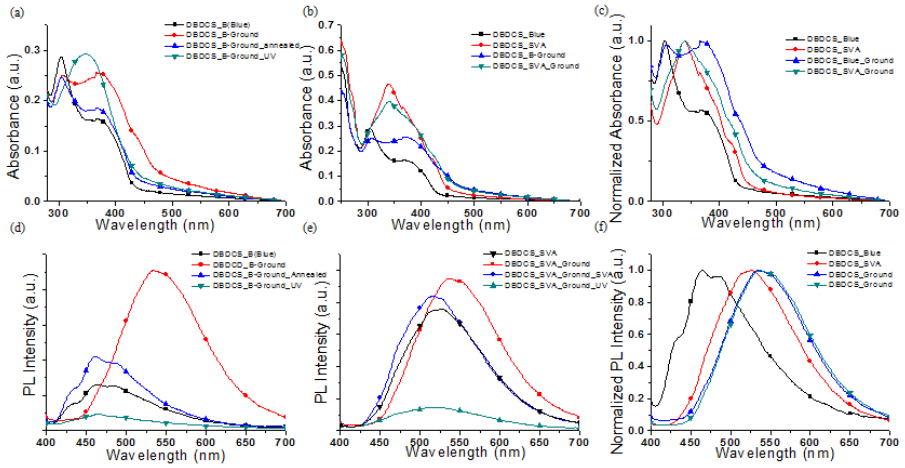

Figure 2.14 UV/PL spectra of DBDCS doped PMMA film. (a),(b),(c) UV absorption and normalized absorption spectrum of the film (d),(e),(f) PL and Normalized PL spectrum of the film

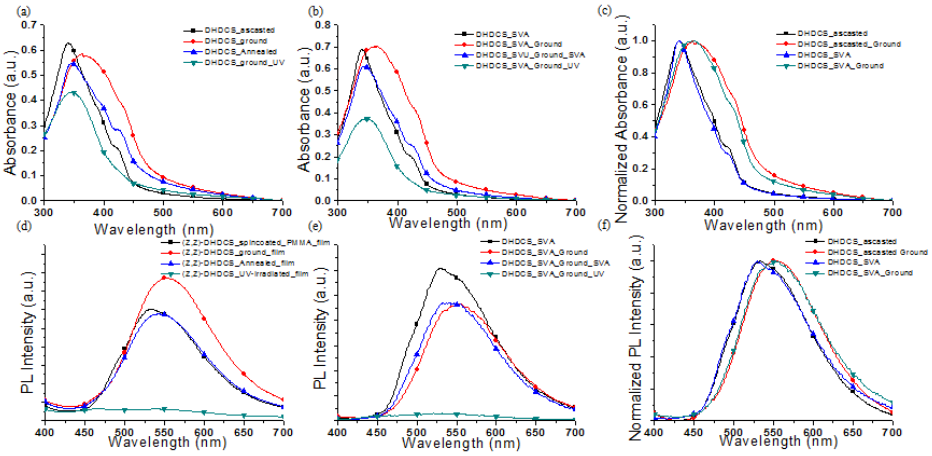

Figure 2.15 UV/PL spectra of DHDCS doped PMMA film. (a),(b),(c) UV absorption and normalized absorption spectrum of the film (d),(e),(f) PL and Normalized PL spectrum of the film.

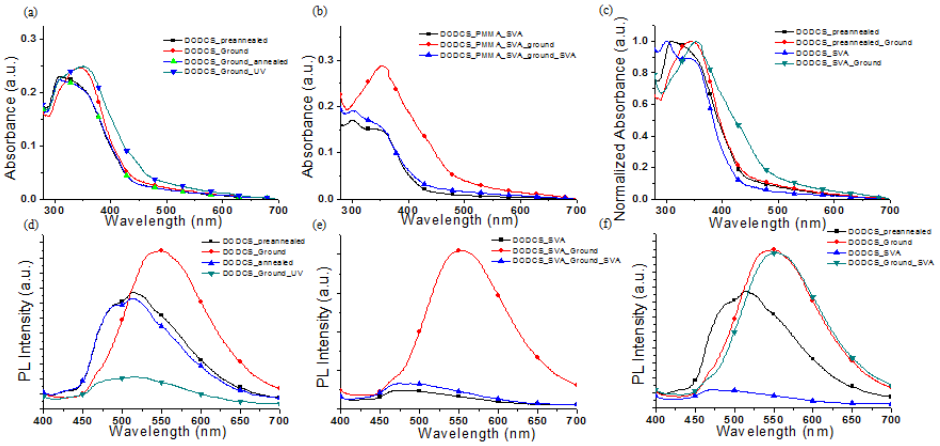

Figure 2.16 UV/PL spectra of DODCS doped PMMA film. (a),(b),(c) UV absorption and normalized absorption spectrum of the film (d),(e),(f) PL and Normalized PL spectrum of the film.

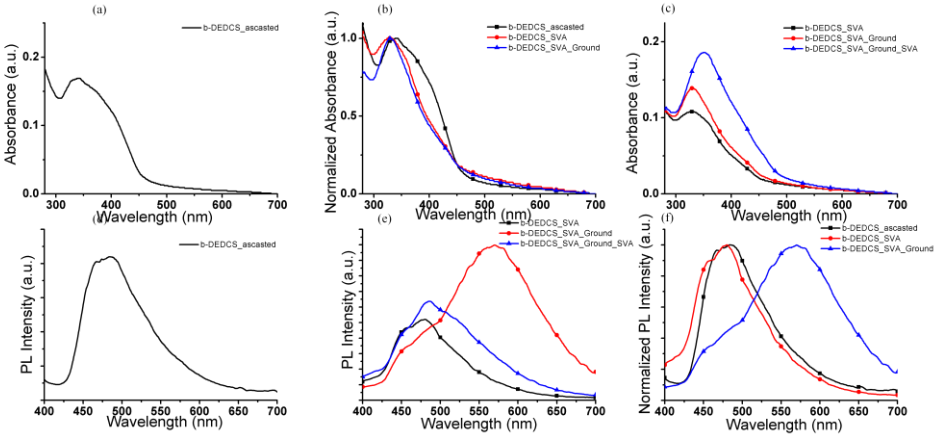

Figure 2.17 UV/PL spectra of β-DEDCS doped PMMA film. (a),(b),(c) UV absorption and normalized absorption spectrum of the film (d),(e),(f) PL and Normalized PL spectrum of the film.

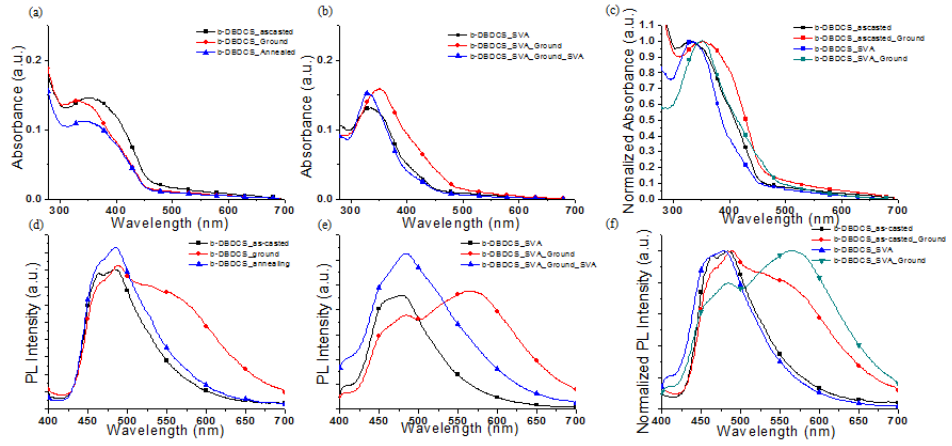

Figure 2.18 UV/PL spectra of β -DBDCS doped PMMA film. (a),(b),(c) UV absorption and normalized absorption spectrum of the film (d),(e),(f) PL and Normalized PL spectrum of the film.

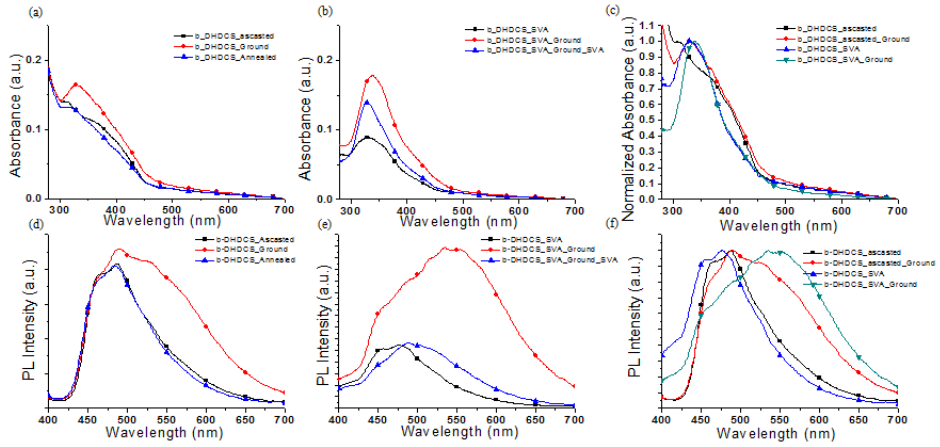

Figure 2.19 UV/PL spectra of β -DHDCS doped PMMA film. (a),(b),(c) UV absorption and normalized absorption spectrum of the film (d),(e),(f) PL and Normalized PL spectrum of the film.

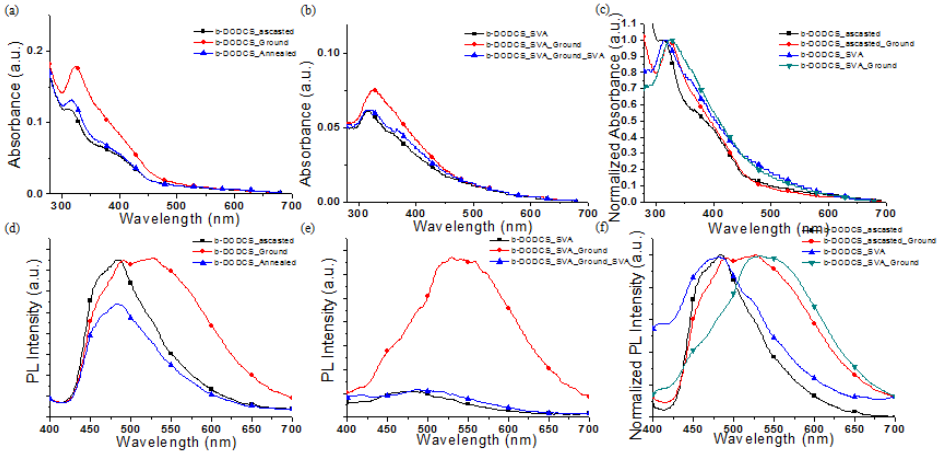

Figure 2.20 UV/PL spectra of β -DODCS doped PMMA film. (a),(b),(c) UV absorption and normalized absorption spectrum of the film (d),(e),(f) PL and Normalized PL spectrum of the film.

2.4 Conclusion

I designed and synthesized eight piezochromic molecules with various length of alkoxy chain and cyano group position. Cyano group can influence electrostatic properties of molecules due to π-conjugation extention. Increase in alkoxy chain does not have affect on photophysical proertiey in solution but have inclination to photophysical properties in solid. However the alkoxy chain plays a important role in not only molecular assembly and fluorescecne in solid state but also stimuli resopnsive behavior. I show piezochromism phenomena of each meterials. By optical properties study in solid film, the reason for altering fluorescence change by mechanical force were explained. Also the materials exhibit vaporchromism with different inclination of fluorescence swiching.

Finally, I firstly reported sequntial piezo- and photo-chromsim phenomena and materials. Fluorescence quenching at smeared films is based on photoisomerzation. I demonstrated fluorescence multi-color patterning in solid state based on dicyanostyrylbenzene type materials via solvent vapor, piezo-writing and photoinduced isomerization. I believe that this research will promote to develop a new class of smart materials in optical device application[1].

2.5 Bibliography

1 a) D. A. Davis , A. Hamilton , J. L. Yang , L. D. Cremar , D. Van Gough ,S. L. Potisek , M. T. Ong , P. V. Braun , T. J. Martinez , S. R. White , J. S. Moore , N. R. Sottos , *Nature* **2009** , *459* , 68 ; b) A. L. Black , J. M. Lenhardt , S. L. Craig , *J. Mater. Chem.* **2011**, *21* , 1655

2. S. Varghese and S. Das, *J.Phys. Chem. Lett*. **2011**, 2, 863-873

3. J.W Chung, Y. You, H. S. Huh, B.-K. An, S. J. Yoon, S. H. Kim, S. W. Lee, and S. Y. Park, *J. Am. Chem. Soc*., **2009**, 131, 8163

4. a) B.-K. An, J. Gierschner, S. Y. Park, *Acc. Chem. Res.* **2011**, *45*, 544; (b) B.-K. An, S.-K. Kwon, S.-D. Jung, S. Y. Park, *J. Am. Chem. Soc.* **2002**, *124*, 14410. (c) S.-J. Yoon, J. W. Chung, J. Gierschner, K. S. Kim, M.-G. Choi, D. Kim, S. Y. Park, *J. Am. Chem. Soc*. **2010**, *132*, 13675

5. (a) C. Lowe, C. Weder, *Adv. Mater*. **2002**, 14, 1625. (b) B.R. Crenshaw, C. Weder, *Chem. Mater*. **2003**, 15, 4717 (c) M. Kinami, B.R. Crenshaw, C.Weder, *Chem. Mater*. **2006,** 18, 946 (d) J. Kunzelman, M. Kinami, B.R. Crenshaw, J.D. Protasiewicz, C. Weder, *Adv. Mater***. 2008**, 20, 1196. (a) Shinto Varghese and Suresh Das, *J.Phys. Chem. Lett*. **2011**, 2, 863 (b) Hong, Ym Lama, J.W.Y, Tang, B. Z, *Chem. Commun*. **2009**,4332 (c) B.-K. An, J. Gierschner, S. Y. Park, *Acc. Chem. Res.* **2011**, *45*, 544

7. S. Kim, S-J. Yoon, S.Y. Park *J.Am. Chem. Soc*. **2012**, 134, 12091

8. S. Wenger, Chem. Rev. **2013**

9. F.J. Lange, M.Leuze, M. Hanack, *J. Phys. Org. Chem*. **2001**, 14, 474

Chapter 3. Photochromic and Piezochromic Fluorescent Materials: Sequential Luminescent Switching via Mechanical and Light Stimuli

3.1 Introduction

Solid-state luminescent switching smart materials, which respond to small changes in their environment with dramatic change of their solid-state luminescent properties, have been intensively investigated due to their potential utilities in memory devices, sensors, security materials, and informational displays[1]. In particular, a promising approach for the research is mechanochromic luminescence which is luminescence reversible switching via force and other stimuli such as heat and solvent vapor. The studies on the fluorescence changes or various emission colors accompanied with molecular assembly present a critical issue because these provide insight into awareness of the role of molecular packing in controlling solid-state optical properties and developing stimuli-sensitive materials[2]. Mechanical forces may induce elongation, deformation, and ruptures of molecules but what phenomena occur at the molecular level is still unclear[3]. Recently, controlling molecular stacking configurations of mechanofluophore is a promising approach for in-depth theoretical understanding of mechanochromic behavior at the molecular level and development novel smart materials. For example, Kato *at el* reported

mechanochromic liquid crystal(LC) which two LC phases in different colors are transform. They developed tricolored mechanochromic LC which is composed of the mixture to generate additional LC phase with additional color[4]. Very recently, Reddy and co-worker have analyzed correlation between the mechanical properties and unusual fast self-healing mechanochromic fluorescence of difluoroboron avobenzone (BF2AVB)[5]. Although their works have shed light on detailed image of molecular events under mechanical force, molecular level understanding of mechanochromism and the development of a novel system has been still limited.

Recently, we and others have demonstrated various stimuli-responsive solid-state luminescent materials incorporating cyanostilbene scaffold as core unit[6]. In fact, cyanostilbene derivatives show distinct characteristics, i.e. (i) aggregation-induced enhanced emission (AIEE) behavior, which improves 'aggregation quenching (AQ)' occurring in common solid-state conjugated molecules[7], (ii) polymorph and polymorph-dependent emission behavior[8], (iii) isomerization E(Z)-form to Z(E)-form, especially in the solid state by UV-light, which enables easy control of solid-state morphology[9] or fluorescence[10], (iv) simple chemical structures and syntheses. These unique features allow cyanostilbene derivative an ideal candidate for stimuli sensitive luminescent smart materials in the solid state.

Herein, we reported a new type of smart materials which show sequential luminescence switching via mechanical and light stimuli. As mentioned in chapter 2, α-dicyanodistyrylbenzene with the end group of alkoxy chain exhibit fluorescence quenching only at mechanically perturbed state. Interestingly, the phenomenon is very different in two different states, pre-annealed and SVA, of DBDCS[5] and DODCS. In DBDCS case, fluorescence quenching is very slow (~12min) in the pre-annealed film and is fast (~150s) in the SVA film (See figure 2.9) under UV irradiation. In contrast, fluorescence quenching occurs only in the pre-annealed DODCS

film against SVA treated DODCS film. The result indicates that UV irradiation time for fluorescence quenching and/or the occurrence of fluorescence quenching is strongly depended on molecular crystal structure, not molecule's intrinsic electrochemical properties. To understand the unique phenomena, we compare DBDCS with DHDCS. Crystal structure in DBDCS is already reported and fluorescence quenching occurred very slowly, while (Z,Z)-DHDCS crystal structure is appreciated and its quenching occurred fastly. Also to understand in-depth knowledge of the mechanism of unique phenomena, we have deeply investigated the structural, electrochemical, and photophysical properties of (Z,Z)-DHDCS system. Notably, we utilized this phenomenon to successfully demonstrate rewritable fluorescent optical recording and ROM recording memory device.

3.2 Experiments

3.2.1 General experimental procedures

(Z,Z)- DHDCS were synthesized according to the procedure shown in Scheme 2.1. All chemicals were purchased commercially, and used without further purification. Synthesis of materials is according to the procedure shown in Chapter 2.2.1. The progress of reation was checked on TLC plate (Merck 5554 Kiesel gel 60 F254) under UV light. Column chromatography was performed on silica gel (Merck 9385 Kiesel gel 60). The solution of (Z,Z)-DHDCS in dicholoromethane shows isomerization under daylight or the radiation of a handled UV lamp. A mixture of the three isomers(Figure 3.1) is obtained from solution under the UV irradiation of handled UV lamp for 12 hour. Isomer mixture of DHDCS is separated by column chromatography on silica-gel using dichloromethane and n-hexane (5:2 v/v).

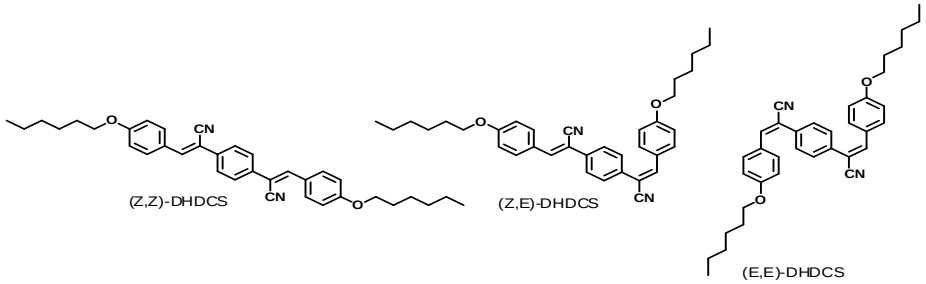

Figure 3.1 Three isomers of DHDCS

(2Z,2'Z)-2,2'-(1,4-phenylene)bis(3-(4-hexyloxyphenyl)acrylonitrile) ((Z,Z)-DHDCS) Green crystallin powder **1H.NMR** (300MHz,CDCl3) δ [ppm]: 7.90(d, 4H), 7.71(s, 4H), 7.51(s, 2H), 6.98(d, 4H), 4.03(t, 4H, -CH2), 1.81(m, 4H), 1.51(m, 4H), 1.36(m,8H), 0.99(t, 6H) **^{13}C NMR** (500MHz,CDCl3) δ [ppm]: 161.36, 142.24, 135.17, 131.40, 126.23, 126.10, 118.31, 114.97, 107.43, 77.26, 77.00, 76.74, 68.30, 31.56, 29.10, 25.68, 22.59, 14.01 HRMS m/z (FAB) calcd. for $C_{36}H_{40}N_2O_2$ (M^+) 532.31, found 532.3083 EA C,81.17% H 7.57; N, 5.26 anal. Calcd. for $C_{36}H_{40}N_2O_2$: C, 81.17; H 7.57; N, 5.26 Found: C, 81.1830: H, 7.5774: N, 5.2151

(2Z,2'E)-2,2'-(1,4-phenylene)bis(3-(4-hexyloxyphenyl)acrylonitrile) ((Z,E)-DHDCS) green powder **1H.NMR** (300MHz,CDCl3) δ [ppm]: 7.89(d, 2H, Ar-H), 7.65(d, 2H, Ar-H), 7.49(d, 2H, Ar-H), 7.46(s, 2H), 7.31(s, 2H), 7.14 (d, 2H), 6.98(d, 2H), 6.75(d, 2H), 4.02(t, 2H,), 3.93(t, 2H), 1.79(m, 4H), 1.541-1.31(broad, 12H), 0.92(q, 6H) **^{13}C NMR** (500MHz,CDCl3) δ [ppm]:

161.41, 160.78, 144.49, 142.61, 135.59, 133.52, 131.66, 129.58, 126.30, 126.03, 125.66, 120.35, 118.30, 114.99, 114.64, 110.51, 107.45, 77.26, 770.00, 76.75, 68.31, 68.19, 31.54, 31.51, 29.10, 29.06, 25.67, 25.64, 22.56, 13.98 (FAB) calcd. for $C_{36}H_{40}N_2O_2$ (M^+) 532.31, found 532.3099

(2E,2'E)-2,2'-(1,4-phenylene)bis(3-(4-hexyloxyphenyl)acrylonitrile) ((E,E)-DHDCS) white powder **1H.NMR** (300MHz,CDCl3) δ [ppm]: 7.41 (s, 4H), 7.31(s, 2H), 7.11(d, 4H), 6.75(d, 4H), 3.93(t, 4H), 1.79(m, 4H), 1.40(m, 4H), 1.34(m, 8H), 0.89(t, 6H) **^{13}C NMR** (500MHz,CDCl3) δ [ppm]: 160.81, 144.79, 133.97, 131.69, 129.68, 125.54, 120.38, 114.62, 110.43, 77.25, 77.00, 76.74, 68.20, 31.52, 29.07, 25.64, 22.55, 13.98 (FAB) calcd. for $C_{36}H_{40}N_2O_2$ (M^+) 532.31, found 532.3096

3.2.2 Sample preparation

Powder sample of (Z,Z)-DHDCS was obtained by recrystallization from ethyl acetate as green crystalline powder. Powder samples of other isomers were just used after column purification and evaporation. Single crystal was grown by slow evaporation methods from ethyl acetate at room temperature. Composite film of DHDCS in PMMA (40 wt%) and of DBDCS in PMMA (20 wt%) were fabricated on quartz or glass substrates by spin casting. Nanoparticles suspensions were obtained by a simple reprecipitation method from DHDCS solution in THF (2 x 10^{-5} mol L^{-1}) by rapidly injection of distilled water in 2:98 volume fraction.

3.2.3 X-ray and Thermal Analysis.

Single-crystal X-ray diffraction data were collected using an Bruker SMART APEX2 ULTRA and a APEX II CCD area detector with a multilayer-monochromated Mo Kα radiation (λ = 0.71073 Å) generated by a rotating anode. Data collection, data reduction, and semiempirical absorption correction were carried out using the software package APEX2. All of the calculations for the structure determination were carried out using the SHELXTL package[11]. All non-H atoms were refined anisotropically. All hydrogen atoms were included in calculated positions with isotropic thermal parameters 1.2 times those of attached atoms.XRD measurements were performed on a Powder X-ray Diffractometry (D8-Advance , Bruker, Germany), operating at 3kW. The thermal properties were investigated using a differential scanning calorimerty (DSC) with TA Instruments and DSC-Q1000 instruments operated at a heating rate of $10^{o}C\ min^{-1}$.

3.2.4 Spectroscopic Characterization.

^{1}H-NMR spectrum was recorded on a Bruker, Avance-300 (300 MHz) in $CDCl_3$ Solution. ^{1}C-NMR was recorded on a Bruker, Avance-500 (500 MHz) in $CDCl_3$ Solution. Mass spectra were recored on JEOL. JMS-700 spectrometer using fast atom bombardment (FAB) method. Significant fragments are reported in the following fashion: m/z (relative intensity). Elemental analysis was carried out using a CE instruments, EA1110 elemental analyzer. UV-visible absorption spectra were recorded on Shimazu, UV- 1650 PC spectrometer. Photoluminescence spectra were obtained using a Photo Technology International, Felix32 QM-4 and a Varian, Cary Eclipse Fluorescence spectrophotometer. The relative fluorescence quantum yield was measured

using quinine sulfate in 1.0N H_2SO_4 as a standard reference ($1x10^{-5}$ mol L^{-1}, $\boldsymbol{\Phi}_F$=53.5%). The absolute $\boldsymbol{\Phi}_F$ values of powder and thin films on quartz plates were measured using a Photo Technology International, Felix32 QM-4 with a 3.5 inch integrating sphere. Time-resolved fluorescence lifetime experiments were performed by the time-correlated single photon counting (TCSPC) technique with a FluoTime200 spectrometer (PicoQuant) equipped with a PicoHarp300 TCSPC board(PicoQuant) and a PMA182 photomuliplier(PicoQuant). The excitation source was a 377nm picoseconds pulsed diode laser (PicoQuant, LDH375) driven by a PDL800-D driver (PicoQuant) with fwhm ~ 70 ps. The muli-exponetial least square fitting procedure was carried out with the Fluofit software (PicoQuant), taking into possible double excitations of the IRF within the deconvolution. Mean decay times τ_{av} were obtained from the individual lifetimes τ_i and amplitudes α_i of muli-exponentail evaluation through

$$\tau_{av} = \frac{\sum_i \alpha_i \tau_i^{\,2}}{\sum_i \alpha_i \tau_i}$$

3.3 Results and discussion

3.3.1 Photoisomerization of (Z,Z)-DHDCS in solid state

With a view of molecular structure, (Z,Z)-DHDCS is very similar to previously reported piezochromic molecules, DBDCS, with only difference in alkyl-chain length. Like DBDCS, (Z,Z)-DHDCS exhibits aggregation-induced enhanced emission behavior, high solid-state fluorescence (Φ_f= 0.77), and green fluorescence emission of nanoparticle suspensions. However, (Z,Z)- DHDCS molecular assemblies behave in very different ways, double action (Figure 3.1), to (Z,Z)-DBDCS system which exhibit traditional two-colored luminescence switching, i.e. blue to green, in response to mechanical stimulus. The first stage is a reversible green to yellow fluorescence switching in response to mechanical and thermal stimuli(Figure 3.1.(b)). The second stage is an irreversible and selective fluorescence 'turn-off' only at mechanically perturbed state, i.e. yellow state, by 365 nm UV-light irradiation. After UV irradiation immediately, the fluorescence is dramatically dimmed (Figure 3.1(c)). Finally, the fluorescence is completely disappeared under 1min (Figure 3.1(e)).

Figure 3.2 Optical microscope image of (Z,Z)-DHDCS. (a) (Z,Z)-DHDCS crystalline powder, (b)-(e)

rolled powder of (Z,Z)-DHDCS under 365nm UV light of Xe lamp depending on the time.

The green fluorescent crystalline powder obtained by recrystallization from ethyl acetate exhibits usual piezochromic behavior. The green luminescence of pristine powder was converted to bright yellowish organge luminescence by rolling it on slide galss (Figure 3.2 (b)). Interestingly, the piezochromic fluorescence was not uniform unlike the general piezochromic materials including (Z,Z)-DBDCS whose two colors or luminrescence are apparently distinguished by naked eyes. We found that piezochromic fluorescence was more red-shifted when the powder was further ground or harder ground. The reversibility of the peizochromism was explored by thermal treatment. Tehn, the powder was kept in the dark (Figure 3.4 and 3.5). After heating the ground powder at 100^{o}C for 10 sec, the original fluorescence was recovered without any chemical reaction. Also the piezochromic fluorescence reverted to the original when the ground powder was kept in the dark over 1 month. The result indicated that piezochromism of (Z,Z)-DHDCS is not only reversible but also self-healable. Moreover, fluorescence quenching was observed only in ground powder under UV-irradiation (λ_{max}=365nm). After the UV treatment, the original or mechanochrmic fluorescence was not restored by thermal annealing.

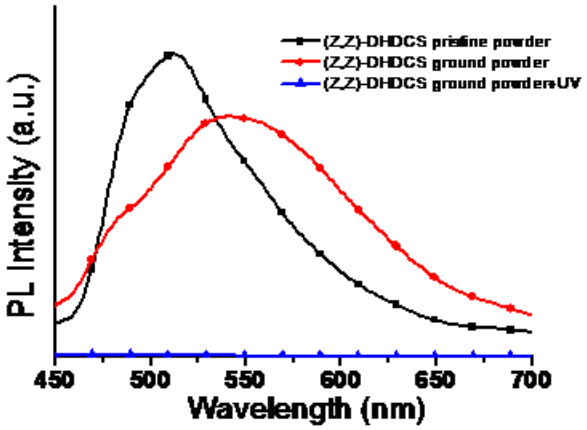

Figure 3.3 PL spectra of (Z,Z)-DHDCS powder samples.

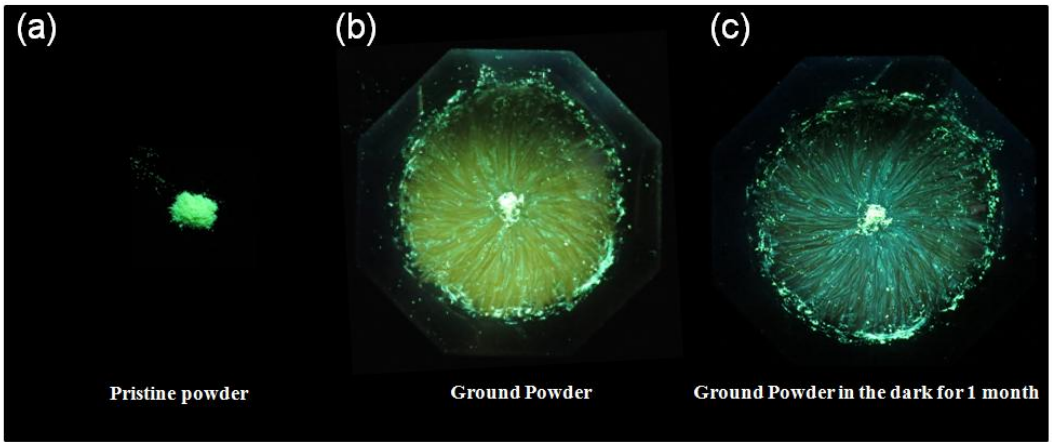

Figure 3.4 Photo of various (Z,Z)-DHDCS powder in a mortar. (a) Pristine crystalline powder (b) ground powder and (c) ground Powder in the dark for 1 month.

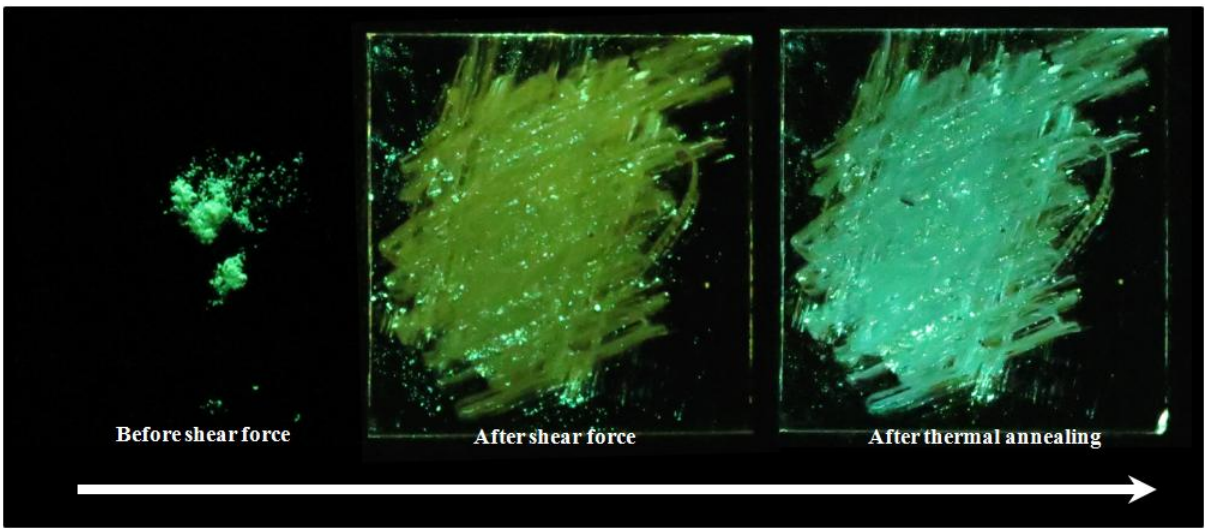

Figure 3.5 Fluorescence changes of (Z,Z)-DHDCS powder by rolling with a glass pipette and thermal annealing.

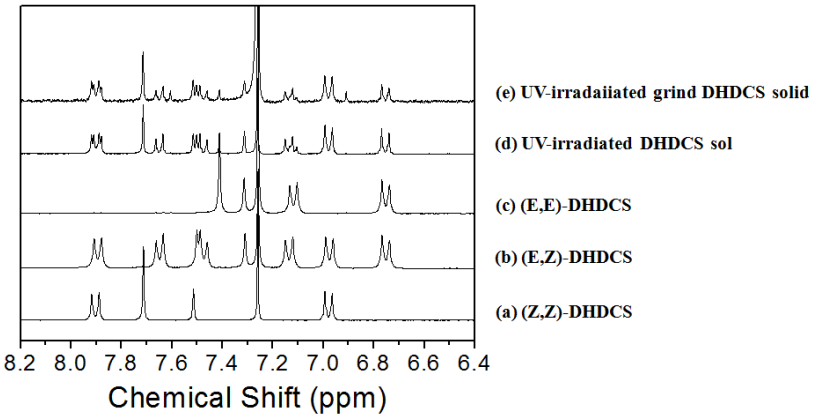

Figure 3.6 ^{1}H-NMR data($CDCl_3$) of DHDCS samples in $CDCl_3$ solution

To understand why fluorescence quenching happens in (Z,Z)-DHDCS powder when the powder was ground under UV-irradiation, I studied on ^{1}H-NMR data. ^{1}H-NMR spectra of ground powder is consistent with that of pristine powder. It means that chemical reaction does not invlove in the piezochromism process. I found that photo induced isomerized (Z,Z)-DHDCS in solution is similar to ground (Z,Z)-DHDCS under UV irradiation in terms of ^{1}H-NMR anaylsis (Figure 3.6). To comfirm that the unique phenomena originate from photo-isomerization, three isomers, (Z,Z)-DHDCS, (Z,E)-DHDCS, (E,E)-DHDCS, were seperated by column purification and were measured on ^{1}H-NMR. The each ^{1}H-NMR peak of ground powder under UV irradiation is perfectly overlapped with that of the sum of three isomers. As a result, such afluorescence quenching event is induced by photoisomerization. Isomer mixture of DHDCS might show non-fluorescence feature.

However, the indepth-theoretical understanding of the phenomena remains still unclear. Moreover, Our group reported that cis-CN-MBE, which is non-fluorescence materials in both solution and solid state, shows fluorescence ‘turn on‘ after UV-irradiation[10]. Tiny amount (5-10%) of trans-CN-MBE, which exhbits aggregation-induced enhanced emission, in Cis-CN-MBE matrix is generated due to photo induced isomerization and emits bright fluorescence. The result of photoisomerization of cis-CN-MBE contradicts the fluorescence quenching phenomena of (Z,Z)-DHDCS. To gain a clear insight of DHDCS phenomena and solve the controversy, I studied on thermal and optical properties and of DHDCS isomer.

3.3.2 Study on photophysical and thermal property of DHDCS isomers

"Photochromism is a reversible transformation of a chemical species induced in one or both directions by absorption of electromagnetic radiation between two forms, A and B, having different absorption spectra"[12]. As shown in Figure 3.5, Cyanostilbenzene in solution shows photoisomerization behavior like stilbene. Upon irradiation with 365 nm UV, the absorption band at 380nm of (Z,Z) DHDCS decreased and new shoulder absorption band at 328nm is appeared. The photo-stationary state (PSS) was reached in about 100 s with isosbestic point at 345nm. In PSS, the absorption shape is almost equal to the spectrum of the 19: 77: 4 ratio configuration of (Z,Z), (Z,E), (E,E) isomers. As shown in Figure 3.4(d)-(f), photo induced isomerized compounds are recovered by heat under N_2 atmosphere. After 1st heating cycle, DSC trace of three compounds is the same which means that thermal isomerization occurs and the isomers become (Z,Z)-DHDCS under 300^{o}C.

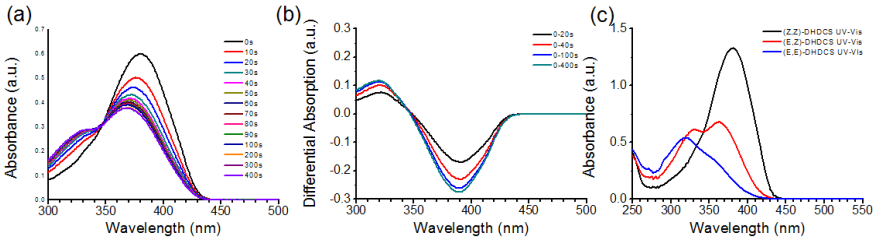

Figure 3.7 (a)-(b) Changes of UV-Vis absorption spectra under 365nm UV-light. (c) Absorption spectra of solutions of DHDCS isomers in THF ($2x10^{-5}$mol L^{-1})

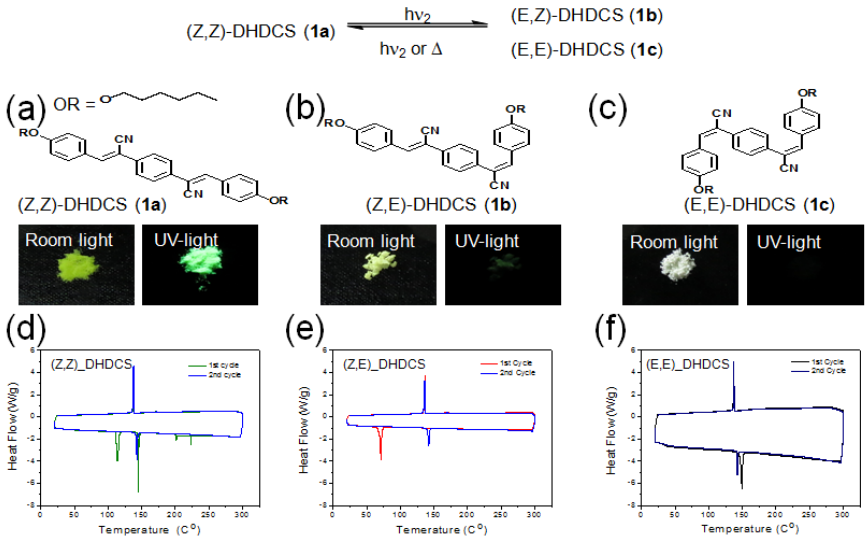

Figure 3.8 (a)-(c) Chemical structures and photo images of powder of (Z,Z), (E,Z), and (E,E)-DHDCS (d)-(f) DSC data of (Z,Z), (Z,E), and (E,E)-DHDCS

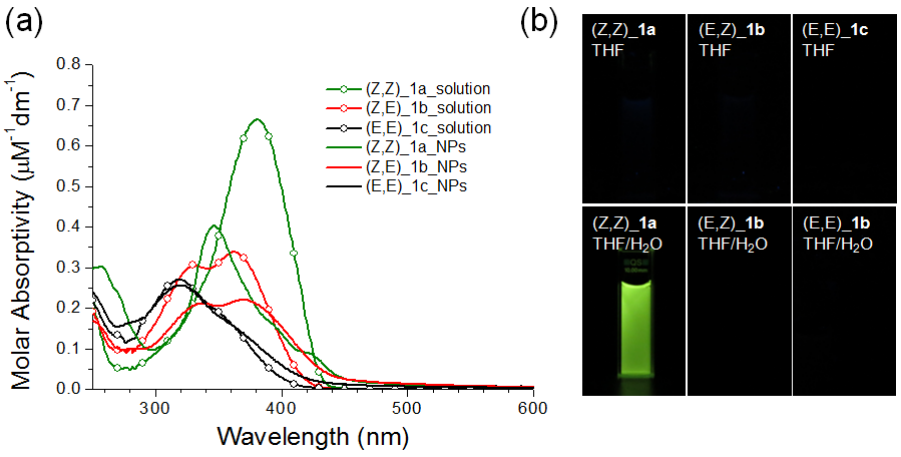

Figure 3.9 (a) Absorption spectra of and (b) photo image of nanoparticle suspensions(THF:H_2O=2:98) and THF solution of DHDCS isomers.

Photophysical properties of isomers in solution and nanoparticle suspension were studied. (Z,Z)-DHDCS absorbs longer wavelength range of UV-Vis light rather than (Z,E)- and (E,E)-DHDCS in solution state due to a linear π-conjugated structure.. In nanoparticles suspensions, structured absorption shape is observed for (Z,Z)-DHDCS. Aggregates of (Z,Z)-DHDCS present H-type aggregation which shows blue-shifted absorption maximum against monomer or solution state. Interestingly, solid-state of (Z,Z)-DHDCS emits strong fluorescence even if the aggregates is H-type(Figure 3.5(b)). The red-shift shoulder absorption peak proves that lowest excitation state of (Z,Z)-DHDCS dimer is not forbidden transition state. Therefore the aggregated nanoparticles emit fluorescence. Compared to (Z,Z)-DHDCS, absorption maximum peak of (Z,E) and (E,E)-DHDCS is blue-shifted. This is because the molecular configuration of (Z,E) and (E,E)-DHDCS is not planer but twisted. The absorption sharp of the isomers in aggregation state is unstructured which means that the aggregates are less electronic-coupled because of their molecular structure. Eventually, (Z,E)- and (E,E)-DHDCS exhibit non-fluorescence in both solution and aggregation state(Figure 3.5(b)).

Surprisingly, I observed some change of (Z,E)- and (E,E)- DHDCS in aggregation state after UV-irradiation. First, Nanoparticles' fluorescence turns on. As shown in Figure 3.6(c), The isomers nanoparticles show non-fluorescence in initial state. After UV irradiation, the nanoparticles emit strong excimeric green fluorescence which is similar to (Z,Z)-nanoparticle in terms of fluorescence shape and PL-life time. The phenomena are also observed in the isomers' powder(Figure 3.7). Based on ^{1}H-NMR analysis, we conformed that (Z,Z)-DHDCS was generated in the isomer nanoparticles. The similar result was previously reported in stilbenzene and cyanostilbenzene[13]. Because to non-planer structure of (Z,E)- and (E,E)-DHDCS, local free volume in crystal could be allowed to undergo photoisomerization in solid state. Therefore, I

conclude that fluorescence of (Z,E)- and (E,E)-DHDCS under UV irradiation originsates from (Z,Z)-DHDCS created by photoisomerization.

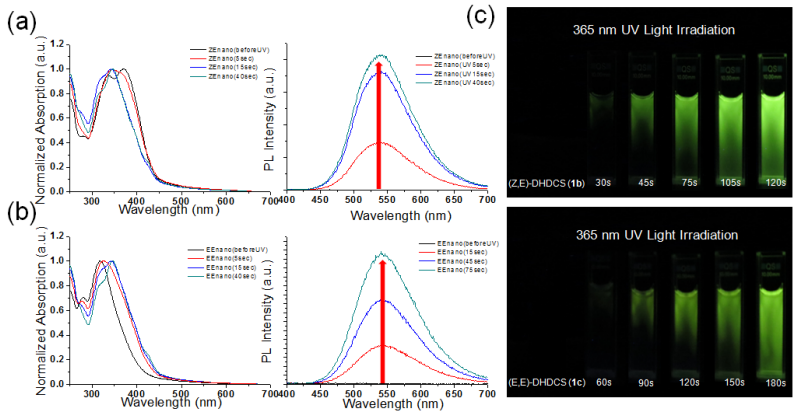

Figure 3.10 (a) UV-Vis/PL spectra of (Z,E)-DHDCS in nanoparticles suspension under UV irradiation depending on the time. (b) UV-Vis/PL spectra of (E,E)-DHDCS in nanoparticles suspension under UV irradiation depending on the time. (c) Photo-image of fluorescence 'turn on' nanoparticles of (Z,E)-and (E,E)-DHDCS.

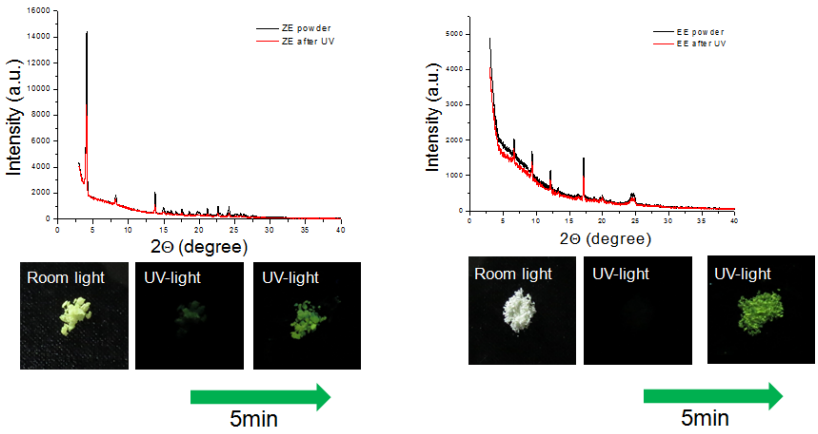

Figure 3.11 XRD data and Photo images of (Z,E)- and (E,E)-DHDCS powder before and after UV irradiation.

Secondly, in absorption spectra unstructured shape was converted to structured shape. In particular, the long wavelength shoulder(~434nm) was appeared. We found that only emissive sample of DHDCS showed absorption shoulder in long wavelength regions like (Z,Z)-DHDCS. Specially, aggregates of (Z,Z)-DHDCS exhibit luminescence and the shoulder. The result means that aggregated (Z,Z) DHDCS is existed in the matrix of each isomers and emited strong fluorescence. Based on UV-vis absorption data, we concluded that some environment factor or the initial state caused to different results. We guess that (Z,E)- and (E,E)-DHDCS powders' crystallinity is little disturbed after UV irradiation. The rigid matrix environment might allow for aggregate (Z,Z)-DHDCS.

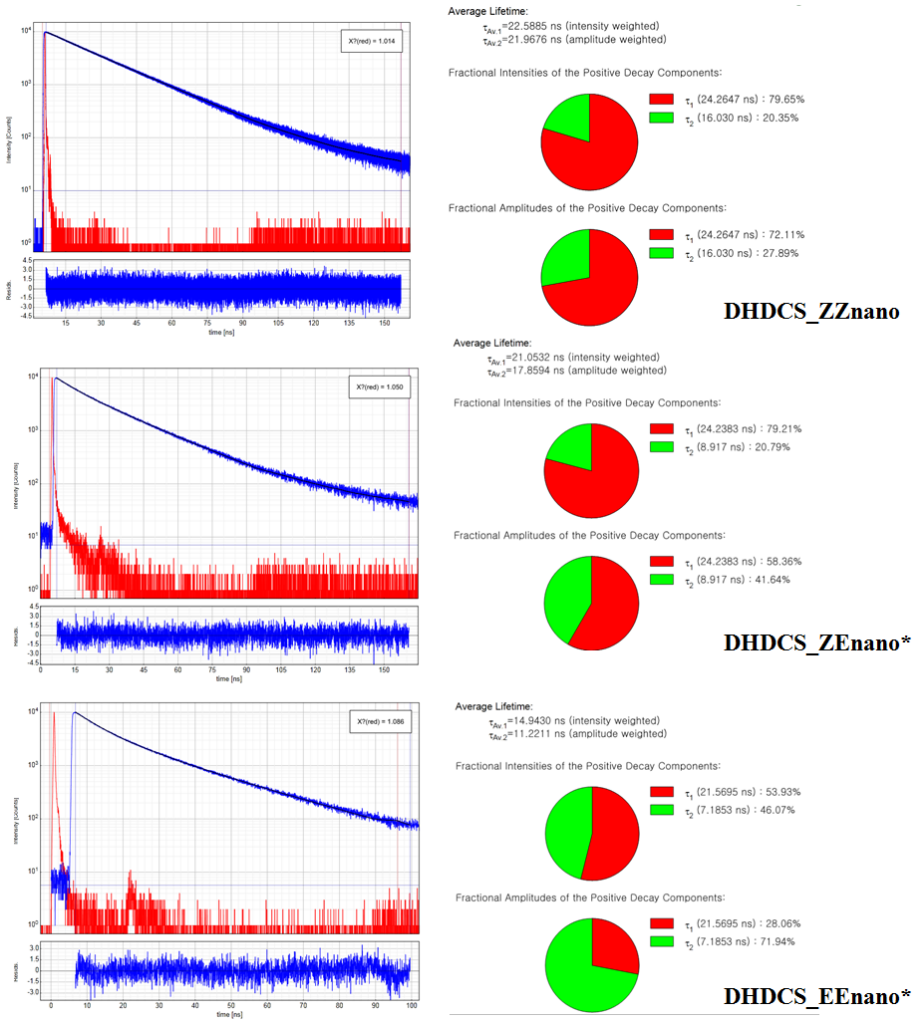

Figure 3.12 Fluorescence decay profiles (upper blue lines) of (Z,Z)-,(Z,E)-, and(E,E)-DHDCS with 377nm excitation. IRFs are presented in red, fits in block; lower blue lines are the residuals.

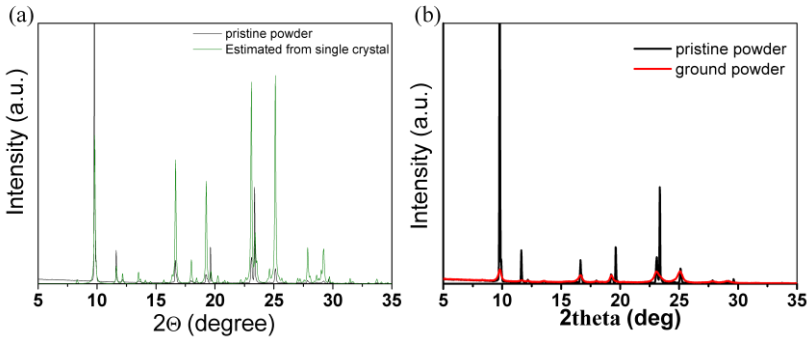

Figure 3.13 XRD data of pristine powder, ground powder, and estimated from single crystal of (Z,Z)-DHDCS.

3.3.3 Single crystal analysis of (Z,Z)-DHDCS and proposed mechanism of piezochromism and fluorescence quenching via photochromism.

It was well reported that photo-isomerization of stilbene or azobenzene occurs in amorphous film, liquid crystal, soft crystalline materials, and specific crystal with some large free volume[9,10,16,17]. To the best of our knowledge, photo-isomerization only in ground powder and the subsequent fluorescence quenching is the first example to show DHDCS in this work. The unique fluorescence 'tune off' phenomena of (Z,Z)-DHDCS could be simply considered that the mechanical force lead to rupture crystal and generate free volume for isomerization. However, photo-isomerization occurs on appropriately oriented void space in crystal but does not in crystal with large total free volume [12]Moreover, we observed that fluorescence change in time difference or the occurrence is dependent on molecular assembly (See Figure S9 in SI). It can be reasonable that the occurrence or lack of photo-isomerization in the ground crystal is associated with the basic of crystal structure. Preference of free void for photo-isomerization might be different based on molecular packing. To gain clear insight of this unique phenomena, we have investigated X-ray crystal structure analysis.

X-ray diffraction (XRD) patterns of (Z,Z)-DHDCS ground powder is quite different from that of (Z,Z)-DHDCS pristine(Figure 4). (i) Several crystalline peaks were disappeared and other became broad. (ii) The specific peak's intensity increase relatively. (iii) Amorphous halo was not observed. There features of XRD patterns implies that deformation occurs in crystal.

The broaden peak indicates decrease in grain size at micro-range during deformation. The slipped crystal lattice was observed on the relatively intensity change of preferred orientation in XRD patterns. Especially, the evidence for remains of crystallinity is the smooth-faced baseline of XRD patterns. We expected that the slipped crystal lattice results in variation of the molecular transition dipole moment interaction and mechanofluorescence. If the crystal lattice is more distorted, the variation of transition dipole moment interaction is larger. This is why (Z,Z)-DHDCS shows piezochromism and further ground powder exhibit more red-shifted luminescent emission.

Single crystal X-ray analysis for (Z,Z)-DHDCS crystal provides additional insight into the mechanism of piezochromism and photochromism in crystal. Figure 5 shows that (Z,Z)-DHDCS molecules consist of the network formed by C-N •••H hydrogen bond and C•••C(π-π) interaction (See green dash lines). In particular, distance of C•••C interaction is only 3.31 Å and the interlayer π-π distance between the adjacent molecules is 3.28 Å. The short distance implies the strong connection with the neighboring molecules a direction perpendicular to the π-surface. The secondary interaction patterns may have a major effect in directing molecular slip[15]. The slip might take place between the networks because of weak and non-directional interaction, van der waals force, between the networks (See yellow dash line and yellow plane in Figure 5a and 5b). We prepared the image of one of the possible slipped molecular stacking (See Figure 5e). Interestingly, the free volumes are located at the top of the molecules' phenyl ring. The site is favorable for π-π inversion which operated during photo-isomerization in stilbene or cyanostilbene. We suggest the most plausible mechanism of fluorescence quenching selectively at mechanically perturbed state under UV-irradiation in (Z,Z)-DHDCS powder that photo-

isomerization occurs in the slip plane due to the enough free space for π-π inversion and destroys the crystal structure. After that, (Z,Z)-DHDCS might not be aggregated in destructed crystal environments and hence the isomer mixture samples exhibited virtually no fluorescence.

The visual evidence for the suggested mechanism was observed in pre-cracked single crystal of (Z,Z)-DHDCS through optical microscope (Figure 6). The triangle shaped crystal was clean and green emissive at first. After observation for 2-3 min under Xe-lamp, the cleavage lines were found and generated gradually quickly. Most uniquely, the cleavage lines were almost parallel to each other. During cleavage line propagation, some cleavage lines were shifted like dislocation glide in metal. We believed that photo-isomerization was initiated in the top edge side of crystal of which crack or pre-deformed lattice existed. The occurrence of photo-isomerization in slip plane induced shear force into lattice and propagated to crack lines in other slip planes. We observed yellow fluorescence in the crystal and loss of polarized character of single crystal during the crack propagation. Interestingly, the only (200) peak with amorphous halo in XRD patterns for the Xe-lamp light irradiated crystal was observed. The peak implies that only long-range orderness is remained in the secondary interaction network assisted to C-N •••H hydrogen bond and π-π interaction as shown in Figure 3.14. It is reasonable that the cleavage lines were slip plane which is located between the networks[11b]. Based on (200) in XRD pattern, we analyzed that the center position of DHDCS molecules was maintained in the network even though molecular motion by photo-isomerization propagated cleavage lines. In contrast, the loss of crystallinity and aggregation is different from UV irradiated (Z,E)- and (E,E)-DHDCS samples. Although the isomers mixture is equal in configuration, (Z,Z)-DHDCS could be aggregated in rigid lattice of (Z,E)- and (E,E)-DHDCS but not in amorphous

environment like UV irradiated ground (Z,Z)-DHDCS powder. The XRD patterns of emissive isomers solid and UV-irradiated the pre-cracked crystal proved our explanation.

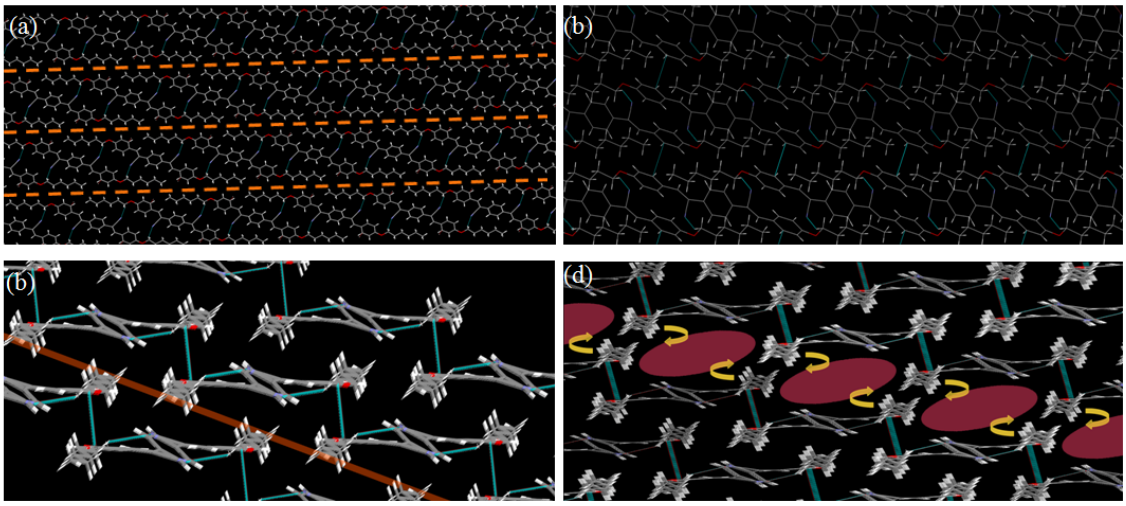

Figure 3.14 (Z,Z) DHDCS molecules in the crystal structure. (a) Top view of a 2D sheet to show C-H •••N interactions. Yellow line is expected to slip plane due to the absence secondary interaction. (b) Side view of 2 sheets. Vertical cyan line shows π-π interaction. (c) Possible molecular structure after grinding (d) Local Free volume site to occur photoisomerization by π-π inversion. Dash line indicates second π-π inversion on the possible free void which is created by π-π inversion.

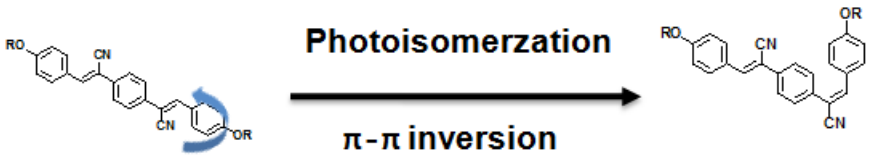

Figure 3.15 Photoisomerization Mechanism of (Z,Z) DHDCS. To occur π-π inversion in solid state, the solid material should be soft or have local free volume.

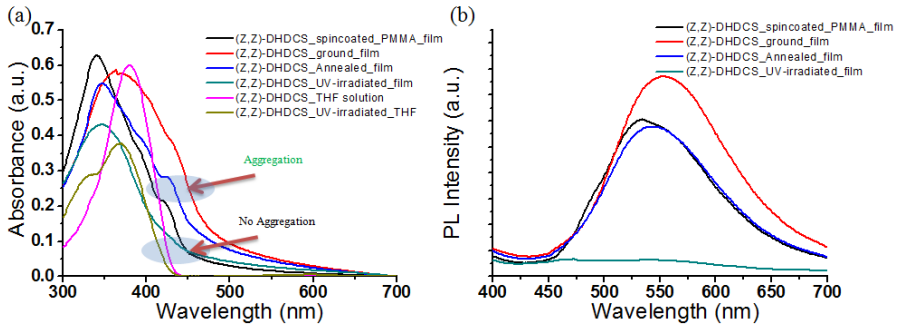

Figure 3.16 UV/PL spectra of (Z,Z)-DHDCS doped PMMA films.

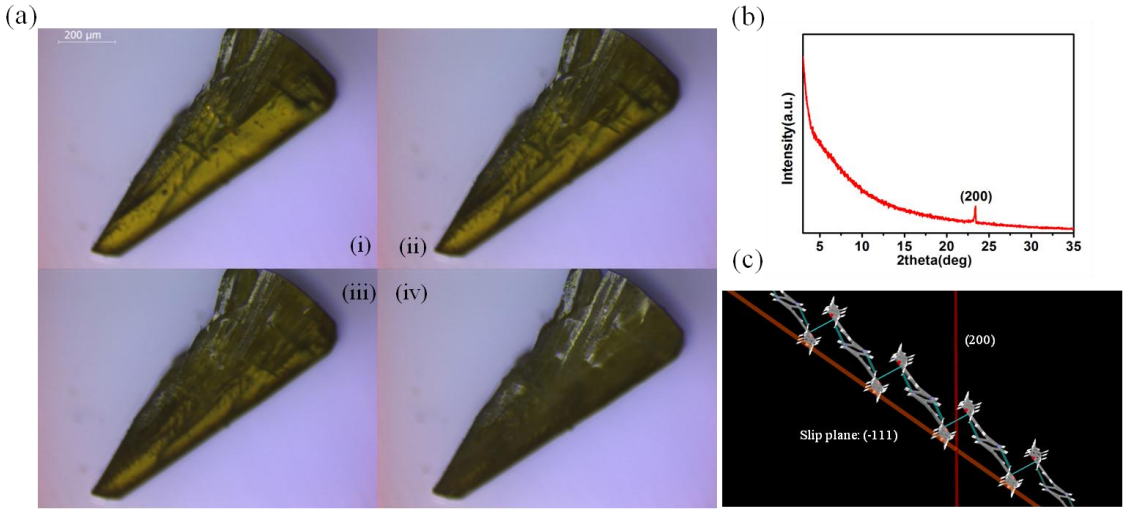

Figure 3.17 (a) Optical Microscope image of pre-cracked (Z,Z)-DHDCS crystal under Xe lamp. (i) through (iv) are listed in chronological order. (b) XRD patterns of (iv) sample. (c) Molecular arrangement in the secondary interaction network of (Z,Z)-DHDCS crystal. Red plane indicates (200) plane.

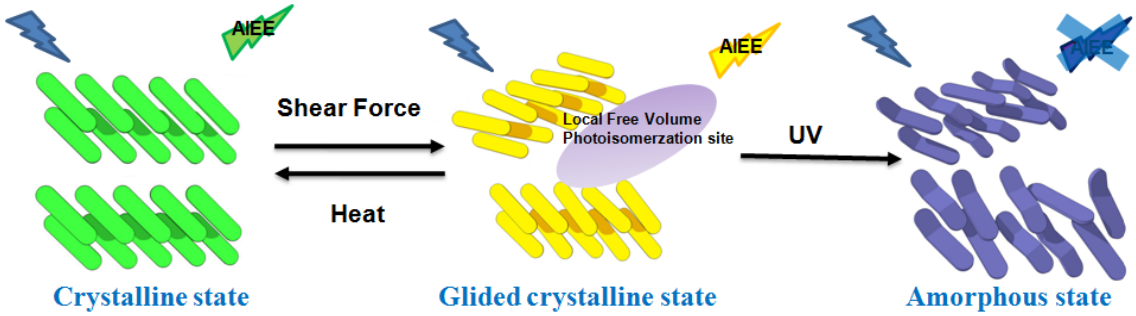

Figure 3.18 Illustration of the possible molecular events in (Z,Z)-DHDCS under external stimulus.

In sum, pristine crystalline powder exhibits a bright green fluorescence. The mechanical force into (Z,Z)-DHDCS pristine powder give rise to slip crystal lattice. (-111) plane is the possible slip plane because (-111) plane is located between molecular network associated by strong secondary interaction such as C-N•••H and C•••C (π---π). During the slip, transition dipole moment interaction distorted and thus fluorescence of powder is red-shifted. Local free volume, is generated, providing a favorable environment for photo-isomerization. After UV-irradiation, photo-isomerization occurs in the local free volume. Molecular motion caused by photo-isomerization induced intermolecular shear force. The intermolecular shear force might lead to additional slipping. Finally, crystal structure is destroyed. UV-irradiated ground (Z,Z)-DHDCS powder could not show fluorescence because (Z,Z)-DHDCS, which is AIEE dyes, could not aggregate in the environments.

3.3.4 Comparison crystal structure of other materials: The working condition of photoisomerzation at the mechanically perturbed state.

In previous chapter 3.3.3, I explained why fluorescence quenching occurs dynamically in (Z,Z)-DHDCS at ground state. However, other piezochromic materials do not show or show slowly the phenomena. For example, fluorescence quenching is very slow in blue-phase of DBDCS. It can be explained that DBDCS's slip plane is π-π plane so that it is not favorable to create local free volume for π-π inversion. The π-π inversion needs enough space upside of flipping phenyl-ring. Even though slip plane is not located on photoisomerization regions, photoisomerzation can occur in some defect created by slip. The amount of the defect might be small so that the resulting defect may be samller, fluorescence quenching is retarding.

As shown in chapter 2, Figure 2.8, β-DCS series do not show the unique phenomena of (Z,Z)-DHDCS. To explore why photo-isomerization behavior in crystal lattice is different, we compared (Z,Z)-DHDCS and β-DBDCS. (Z,Z)-DHDCS molecules are arranged along the long molecular axis with a counter pitch angle of 22.6^{o}. Due to large slipped crystal structure, free volume is created into up and down site of molecules when the crystal is slipped. In contrast, β-DBDCS is less slipped against (Z,Z)-DHDCS. The counter pitch angle is 72.6^{o}. Also the motif in crystal system is dimer that connects strongly each other by hydrogen bonding. As shown in Figure 3.15(a)-(e), expected slip plane is located between networks of hydrogen bonding. It is obvious that mechanical force deforms or ruptures crystal in the slip plane but cannot generate free volume for photoisomerization. The result implies that slip angle is very important for photoisomerization at ground state.

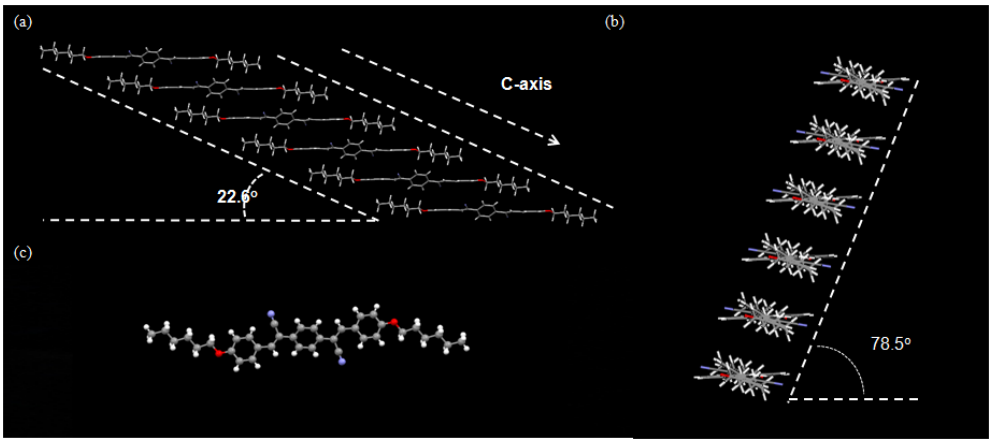

Figure 3.19 Crystal structure of (Z,Z)-DHDCS. (a) Side view and illustration of counter pitch angle. (b) Front view and illustration of counter roll angle. (c) The motif of the crystal system.

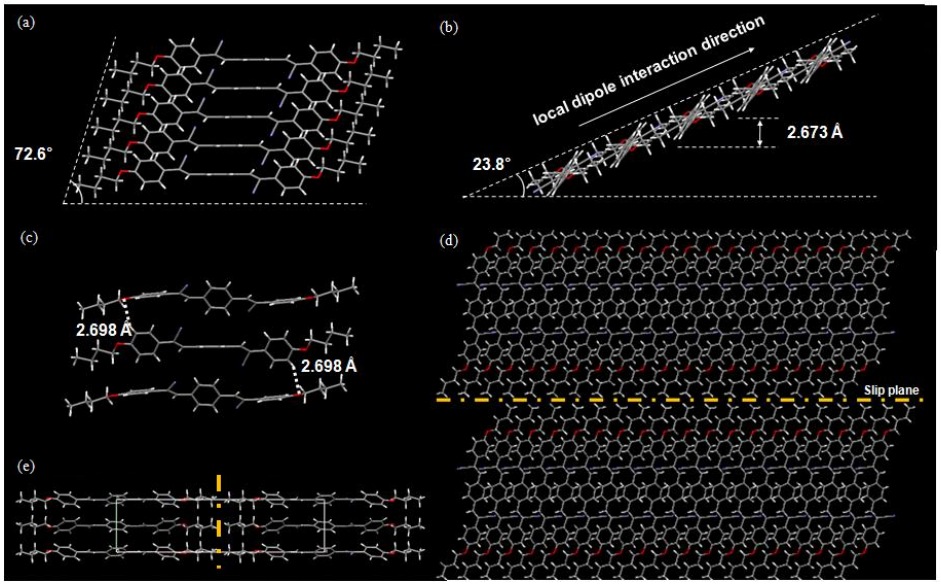

Figure 3.20 Crystal structure of β-DBDCS. (a) Side view and illustration of counter pitch angle. (b) Front view and illustration of counter roll angle. (c) Side view and illustration of he motif of the crystal system. (d) Top view and illustration of slip plane. (e) side view and illustration of slip plane.

3.3.5 Highly fluorescence tri-colored switching luminescence writing via sequential mechanical and light stimuli

As already discussed in previous part, the fluorescence switching experiment was conducted by using (Z,Z)-DHDCS. The thin film was fabricated on quartz by spin-coating method (1000 rpm, 30s). The solution for spin-coating was prepared with 1g of THF, 35mg of PMMA, and 12mg (Z,Z)-DHDCS. The spin-casted film showed highly pressure-sensitivity, changing green emission to yellow with mechanical shear force, which is piezo-writing. When thermal annealing was applied for 30s at 100^{o}C with hot plate, the original color, green was recovered. Upon exposing UV-irradiation at the mechanically perturbed state for 10 sec, yellow luminescence emissive patterns were dimmed. After 90s, yellow emissive color was selectively disappeared. Therefore, the film can be used for not only reversible piezo-writing and thermal-erasing but also permanently patterns at selective region. Therefore I demonstrate multi-stimuli responsive tri-colored luminescence switching smart materials.

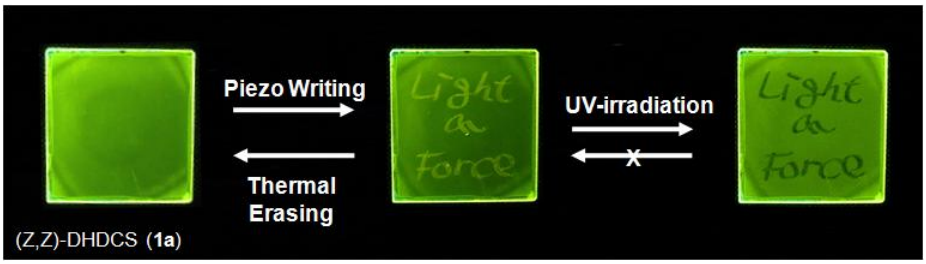

Figure 3.21 Dual action of (Z,Z)-DHDCS doped PMMA film

3.4 Conclusion

In summary, I have reported the unique phenomenon, photo-isomerization only in mechanically perturbed crystal, and their luminescent changes for solid-state (Z,Z)-DHDCS. On the basis of optical, photo-physical, and structural studies, I realized the most plausible mechanism that shear force induces to slip crystal lattice and photo-isomerization occurs in between the network associated C-N•••H and irregularly strong π- π interaction. By correlation between structure and optical properties, how to change fluorescence via mechanical and light stimuli was explained. We visualized the process of photo-isomerization in solid-state by observing the parallel crack propagation in pre-cracked crystal under Xe-lamp. Also, compared to other dicyanostylybenzene, we explain why the fluorescence quenching time and/or the occurrence of fluorescence quenching is different from molecular assembly. Finally, we utilized this phenomenon to demonstrate rewritable and read-out-only accessible fluorescent optical recording media which exhibit sequential luminescence switching via mechanical and light stimuli.

3.5 Bibliograrphy

1. a) Y. Sagara , T. Kato , *Nat. Chem.* **2009** , *1* , 605 ; b) Z. Chi , X. Zhang ,B. Xu , X. Zhou , C. Ma , Y. Zhang , S. Liu , J. Xu , *Chem. Soc. Rev.* **2012** , *41* , 3878 ; c) A. Pucci , G. Ruggeri , *J. Mater. Chem.* **2011** , *21* , 8282 ; d) K. Ariga , T. Mori , J. P. Hill , *Adv. Mater.* **2012** , *24* , 158 .

2. S. Varghese and S. Das, *J.Phys. Chem. Lett*. **2011**, 2, 863

3. K. Ariga, T. Mori, and J. P. Hill *Adv.Mater.* **2012**, 24, 2, 158

4. (a) Y. Sagara, T. Kato *Angew. Chem*. **2011**, 123, 9294 (b) Y. Sagara, T. Kato, *Nat. Chem*. **2009**, 1, 605 – 610. (c) Y. Sagara, T. Kato, *Angew. Chem*. **2008**, 120, 5253; *Angew. Chem. Int. Ed***. 2008**, 47, 5175 – 5178

5. (a) G. Zhaung, J. Lu, M. Sabat, C.L. Fraser, *J. Am. Chem. Soc*. 2012, 132, 2160 (b) G.R. Krishna, M. S.R.N. Kiran, C.L. Fraser, U. Ramamurty, and C.M. Reddy *Adv. Mater*. **2013**, 23, 11, 1422

6. (a) B.-K. An, S.-K. Kwon, S.-D. Jung, S. Y. Park, *J. Am. Chem. Soc*. **2002**, 124, 14410. (b)B-K An, D-S Lee, J-S Lee, Y-S Park, H-S Song, S.Y. Park, *J. Am. Chem. Soc*. **2004**, 126, 11154 (c) B-K. An, S.H. Gihm, J.W. Chung, C.R. Park, S-K. Kwon, S.Y. Park. *J. Am. Chem. Soc.* **2009**, *131*, 3950

7. B.-K. An, J. Gierschner, S. Y. Park, *Acc. Chem. Res.* **2011**, *45*, 544;

8. S.-J. Yoon, J. W. Chung, J. Gierschner, K. S. Kim, M.-G. Choi, D. Kim, S. Y. Park, *J.*

Am. Chem. Soc. **2010**, *132*, 13675

9. 박진욱(**2012**), "고형광성 사이아노스틸벤 파생물들을 기반으로 한 새로운 광반응 연성재료: 광물리적 특성, 액정, 그리고 광화학 상 변화 거동에 대한 연구**"**, 서울대 공학석사 학위논문

10 J.W Chung, S-J Yoon, B-K An, and S. Y Park, "High Contrast On/Off Fluorescence Swithing Via Reversible Trans-Cis Isomerization of α-Cyanostilbene", submitted.

11. (a) APEX2 (Version 2009.1−0) Data Collection and Processing Software; Bruker AXS Inc.: Madison, Wisconsin, U.S.A., **2008**. (b) SHELXTL-PC (Version 6.22) Program for Solution and Refinement of Crystal Structures; Bruker AXS Inc.: Madison, Wisconsin, U.S.A., **2001**.

12. H. Durr and H. B-L(Eds.) (Studies in Organic Chemistry 40), *Elsevier, Amsterdam*, **1990**, 1068

13. J.N. Moorthy, P. Venkatakrishnan, G. Savitha, R.G. Weiss, *Photochem. Photobiol. Sci*., **2006**, 5, 903

14.J. Gierschner, M. Ehni, H. Egelhaaf, B. Milia´n Medina, D. Beljonne, H. Benmansour, G.C. Bazan,. *J. Chem. Phys.* **2005**, *123*, 144914.

15. S. Varughese, M.S.R.N. Kian, U. Ramamurty, G.R. *Desiraju Angew. Chem. Int. Ed*. **2013**, 52, 2701

16. J.N. Moorthy, P. Venkatakrishnan, G. Savitha, R.G. Weiss, *Photochem. Photobiol. Sci*., **2006**, 5, 903

17 Y. Okui, M. Han, *Chem. Commun*. **2012**, 48, 11763

초 록

고형광성 다이사이아노스틸벤 파생물들을 기반의 새로운 압력변색성 광응답성 스마트형광소재: 광물리적 특성, 자극에 의한 광 변화, 그리고 결정구조에 대한 연구

정재훈

재료공학부

The Graduate School

Seoul National University

고상에서 기계적 자극에 반응하는 유기 물질은 결정공학과 형광감응센서, 광메모리 소자, 암호 종이소재 등의 다양한 범위의 응용성 때문에

전도유망한 연구주제이다. 이 분야에 대한 집중적인 연구에도 불구하고, 분자조립과 그에 대한 광특성 조절에 대한 분자설계 전략은 거의 없다. 또한 분자조립 변화에 따른 발광변화에 대한 분자영역에서의 이론적인 이해와 분자구조와 광특성의 관계에 대한 이해는 여전히 불분명하다. 최근 분자조립이 고상에서 파이공액분자 광특성에 미치는 역할을 이해하기 위해 수많은 압력변색성 물질들이 보고되고 연구되고 있다. 그럼에도 불구하고 아직까지 오직 몇몇 그룹만이 결정구조와 광특성 관계와 구조변화 매커니즘에 대해 성공적으로 설명하였다.

본인은 새로운 종류의 알파-다이사이아노스틸벤젠 유도체들에 대해 보고한다. 이 유도체들은 다음과 같은 특징을 보인다. (i) 용액상태에서 형광이 없지만 고상상태에서 강한 형광을 보이는 특성 (AIEE) (ii) 다형결정구조와 다형결정구조에 기인하는 발광 특성 (iii)기계적 자극과 용매 증기 자극에 의한 형광 변화와 열에 의한 회복 (iv) E(Z)-형에서 Z(E)-형 변화의 이성질체화, 특히 자외선 조사상태에서 기계적 힘을 받은 고상 부분의 이성질체화. 분자들의 구조는 알킬 체인 길이와 사이아노기의 위치를 제외하고 같다. 이들 분자의 태생적인 광물리적 특성을 결정하는 분자 뼈대가 같지만, 고상에서 광특성과 자극에 의한 반응 특성이 매우 다르다. 이런 관점에서 고상에서 다양한 광특성을 이해하기 위해 다음과

같은 관점에서 연구를 진행하였다. (i) 알킬 체인 길이와 사이아노기 위치가 결정구조와 광특성을 조절하는 역할 (ii) 기계적 자극을 가한 부분에서 형광소멸의 매커니즘에 대한 이해. 나는 결정분석과 광물리특성 평가, XRD와 ^{1}N-NMR을 통해 위 현상의 가장 가능성있는 매커니즘을 제안하고 구조와 광특성의 관계에 대한 이론적인 설명을 하였다. 마지막으로 가역적인 압력변색기록과 비가역적인 read-out-only가 가능한 메모리 소자를 선보였다.

주요어: 다이사이아노시틸벤젠, 압력변색성, 기계적힘에 의한 변색성, 분자조립, 광이성질체화, 형광기록, 결정공학

학 번: 2011-24050

List of Presentation

1. Jaehoon Jung, Min Sang Kwon, Jong Hyun Kim, Jong Won Chung, and Soo Young Park , "Synthesis and property of new oligothiophene derivative with electron-withdrawing groups“, KJF International Conference 2011 on Organic Materials for Electronic and Photonics, September 15, 2011, Kyeongju

2. Jaehun Jung, Min Sang Kwon,and Soo Young Park, "Fluorescent Photochromic Molecule: sequential luminescene switching via mechanical and light stimuli“, Korea-France Joint Symposium Collocated with CNRS-EWHA, February 1, 2013, Ewha Womans University

감사의 글

CSOM에서 일하는 동안 수많은 고생을 하였지만, 한편으로 제 삶을 풍성하게 채워준 것 같습니다. 돌이켜보면 어렵고 힘들었던 시간들이 다시 돌아오지 않을 즐겁고 소중한 시간이었던 것 같습니다. 제가 겪었던 어려움과 경험들이 훗날 제 삶의 추억과 훈장으로 빛나게 되리라 생각합니다. 이 기간 동안 많은 분들의 도움을 받았기에 지금의 제가 존재할 수 있었습니다. 이 지면을 빌어 짧게 감사의 마음을 표하고자 합니다.

먼저 가장 오랜 시간 실험실에서 함께한 CSOM 구성원들께 감사 드립니다. 나의 장난을 잘 받아준 상훈이, 티격태격 했던 명현이, 친구 같았던 동생 정욱이, 같이 공부 많이 했던 종하, 잘나가는 상규,친절한 원식이, 동생을 잘 챙겨주던 종현이형, 밥 많이 사준 동렬이형, 저의 첫 사수 언스형, 상냥한 일훈이 형, 이것 저것 잘 가르쳐준 성준이 형, 꼼꼼아 정아, 섬세한 혜연이, 말없는 부장 정화, 형이랑 친해지고 싶었던 상윤이, 덜렁이 영주, 몰래 공부다 해놓는 도진, 부사수 같은 내 동생 형주, 학부 때부터 친해지고 싶었던 멋진 해림이, 모두 고맙습니다. 진홍이에게는 이것저것 부탁을 많이 했었던거 같은데 형이 미안하고 또 고마웠다. 특히 우리 빛 나는 AIEE 팀, 민상아 너는 나의 사수이기 전에 30살 근처에 새로 사귈 수 있었던 첫 영혼의 친구였다. 너에게 정말 여러가지로 많이 고마워. 내 옆자리에 앉아 있던 귀여운 동생 진욱이, 형의 실험이야기 많이 들어줘서 고생 많았다. 이쁜 민아, 글씨 이쁘게 써줘서 고맙고 너 덕분에 실험실 여학우들과 친해진 것 같다. 무심한 오빠 많

이 챙겨줘서 고마워. 서장원 박사님, 정말 감사 드립니다. 박사님 덕분에 무사졸업 한 것 같아요. 실험 외적인 것으로도 많은 은혜를 입었습니다. 정말 감사 드립니다. 내 동생 지원이, 형이 뭐 놀릴 구석이 있다고 구박하니, 그래도 너가 있었기에우리 Psudo AIEE 똑똑하고 잘 생긴 영원한 부방장 종한이, 애드워드 유승찬이와 함께 즐거운 CSOM 생활을 좀 더 즐겁게 보낼 수 있었어. 또 CSOM의 오래된 졸업생 봉기형, 정종원 박사님, 저에게 주신 관심과 사랑 덕분에 더 큰 꿈을 가지게 된 것 같습니다. 부족한 글 솜씨에 감사의 마음을 모두 표하지 못해 죄송합니다. 항상 그래왔듯이 CSOM 구성원들이 힘을 합쳐 계속 창의적인 연구를 하고 좋은 성과가 있기를 진심으로 바랍니다.

저를 묵묵히 지켜봐 주신 부모님 감사합니다. 일찍 집에 들어오는 친구 대학원생 아들과 저를 비교하시는 부모님. 집에 와서 같이 저녁식사 많이 하지 못해서 죄송합니다. 아들과 함께 시간을 보내고 싶은 아버지, 어머니의 마음 알아주지 못해서 죄송합니다. 오랜 연애 기간 동안 데이트도 제대로 못한 나의 아내, 안나. 기다려줘서 고마워. 앞으로 우리의 삶이 어려워지고 힘들어지더라도 너에 대한 나의 마음 변치 않고 사랑해줄께.

마지막으로 저의 부족한 점을 많이 지적하시고 지도해주신 박수영 교수님께 감사 드립니다. 학업에 항상 성공을 해왔기에 기가 충분한 저를 자만하지 않고 더 발전하고 나아갈 수 있도록, 자상하신 배려, 격려의 한 마디 한 마디가 큰 힘이 되었습니다. 앞으로도 사회에 나가서 교수님 제자로서 부끄럽지 않게 활동하고 교수님의 명예와 자랑이 되도록 살겠습니다. 그리고 바쁘신 와중에도 저의 부족한 논문 심사

를 허락해주신 김장주 교수님, 김재필 교수님께도 감사 드립니다.

끝은 언제나 또 다른 시작이라고 합니다. 제가 새로운 출발을 할 수 있도록 도움을 주신 많은 분들께 다시 한번 감사의 말씀을 전합니다.